

RECOVERY ACT: Geologic Sequestration Training and Research

Final Scientific/Technical Report

Reporting Period Start Date: December 1, 2009

Reporting Period End Date: June 30, 2013

Peter M. Walsh,* Richard A. Esposito,†* Konstantinos Theodorou,‡*
Michael J. Hannon, Jr.,* Aaron D. Lamplugh,§* and Kirk M. Ellison†*

*University of Alabama at Birmingham

†Southern Company, Birmingham, AL

‡Jefferson State Community College, Birmingham, AL

§John A. Volpe National Transportation Systems Center, Cambridge, MA

Date Report Issued: December 17, 2013

DOE Award Number DE-FE0002224

Submitted by:

University of Alabama at Birmingham
Department of Mechanical Engineering

BEC 257

1720 2nd Avenue South
Birmingham, AL 35294-4461

Disclaimer

This report was prepared as an account of work sponsored by an agency of the United States Government. Neither the United States Government nor any agency thereof, nor any of their employees, makes any warranty, express or implied, or assumes any legal liability or responsibility for the accuracy, completeness, or usefulness of any information, apparatus, product, or process disclosed, or represents that its use would not infringe privately owned rights. Reference herein to any specific commercial product, process, or service by trade name, trademark, manufacturer, or otherwise does not necessarily constitute or imply its endorsement, recommendation, or favoring by the United States Government or any agency thereof. The views and opinions of authors expressed herein do not necessarily state or reflect those of the United States Government or any agency thereof.

Abstract

Work under the project entitled "Geologic Sequestration Training and Research," was performed by the University of Alabama at Birmingham and Southern Company from December 1, 2009, to June 30, 2013. The emphasis was on training of students and faculty through research on topics central to further development, demonstration, and commercialization of carbon capture, utilization, and storage (CCUS). The project had the following components: (1) establishment of a laboratory for measurement of rock properties, (2) evaluation of the sealing capacity of caprocks, (3) evaluation of porosity, permeability, and storage capacity of reservoirs, (4) simulation of CO₂ migration and trapping in storage reservoirs and seepage through seal layers, (5) education and training of students through independent research on rock properties and reservoir simulation, and (6) development of an advanced undergraduate/graduate level course on coal combustion and gasification, climate change, and carbon sequestration.

Four graduate students and one undergraduate student participated in the project. Two were awarded Ph.D. degrees for their work, the first in December 2010 and the second in August 2013. A third graduate student has proposed research on an advanced technique for measurement of porosity and permeability, and has been admitted to candidacy for the Ph.D. The fourth graduate student is preparing his proposal for research on CCUS and solid waste management. The undergraduate student performed experimental measurements on caprock and reservoir rock samples and received his B.S.M.E. degree in May 2012.

The "Caprock Integrity Laboratory," established with support from the present project, is fully functional and equipped for measurement of porosity, permeability, minimum capillary displacement pressure, and effective permeability to gas in the presence of wetting phases. Measurements are made at ambient temperature and under reservoir conditions, including supercritical CO₂. During the course of the project, properties of 19 samples provided by partners on companion projects supported by NETL were measured, covering a range of permeabilities from 0.28 mdarcy to 81 mdarcy.

Reservoir simulations were performed for injection of 530,000 tonnes of CO₂ through a single well into the Middle Donovan formation in Citronelle Dome, in southwest Alabama, over 40 years, followed by migration and trapping for 10,000 years, using the TOUGH2 and TOUGHREACT software packages from Lawrence Berkeley National Laboratory. It was estimated that 50 kg CO₂/m³ of formation would be converted to mineral phases within the CO₂ plume during that time. None of the sand units considered for CO₂ storage in Citronelle Dome have thickness exceeding the estimated critical CO₂ column height (Berg, 1975) at which seepage might begin, through their confining shale layers. A model for leakage through caprock, based on work by Hildenbrand et al. (2004), including a functional relationship between capillary pressure and the effective permeability to gas in the presence of a wetting phase, demonstrated the sensitivity of long-term storage to caprock permeability and thickness.

A traditional course on coal combustion was augmented with material on climate change, coal gasification, and carbon sequestration. A total of 49 students completed the course during two offerings, in Fall 2010 and Fall 2012. It has become a popular advanced elective course in the Department of Mechanical Engineering.

Acknowledgments

The material presented in this report is based upon work supported by the U. S. Department of Energy under American Recovery and Reinvestment Act Award Number DE-FE0002224, entitled, "Geologic Sequestration Training and Research," and by the Alabama Power Company and Southern Company, under the project entitled, "Geologic Carbon Sequestration: Caprock Integrity Laboratory." The measurements of porosity, permeability, and minimum capillary displacement pressure are also supported by Montana State University under Award Number DE-FE0004478 from the National Energy Technology Laboratory, entitled: "Advanced CO₂ Leakage Mitigation using Engineered Biomineralization Sealing Technologies," and by Advanced Resources International under Award Number DE-FE-0010554 from the National Energy Technology Laboratory, entitled: "Commercial Scale CO₂ Injection and Optimization of Storage Capacity in the Southeastern United States."

The authors thank Jack C. Pashin at the Geological Survey of Alabama (Dr. Pashin is now at Oklahoma State University), Shawna Cyphers of Advanced Resources International, and Adrienne J. Phillips, Ellen G. Lauchnor, and Alfred B. Cunningham in the Center for Biofilm Engineering at Montana State University, for providing rock samples for testing and valuable advice on equipment and procedures for measurement of single- and two-phase permeabilities of reservoir rock and caprock. The samples provided by Jack Pashin were from drill core collected during work under the SECARB Phase II Black Warrior Basin Coal Seam Project. Those provided by Shawna Cyphers were from drill core collected during preparation for the SECARB Phase III Anthropogenic CO₂ Injection Field Test. The samples provided by Adrienne Phillips and Al Cunningham were practice, control, and biomineralized cores from the project entitled, "Advanced CO₂ Leakage Mitigation using Engineered Biomineralization Sealing Technologies." Those provided by Ellen Lauchnor and Al Cunningham were candidates for biomineralization under the "Advanced CO₂ Leakage Mitigation" project. The authors are grateful to all of these partners for their generous sharing of valuable samples and expertise.

The Principal Investigator (PMW) thanks Brian W. Dressel for his very helpful and effective collaboration as NETL Project Manager.

The authors acknowledge, with gratitude, the contributions of the National Energy Technology Laboratory, Alabama Power Company, and Southern Company to the Caprock Integrity Laboratory at UAB.

Contents

Disclaimer	ii
Abstract	iii
Acknowledgments	iv
List of Tables	vi
List of Figures	vii
Executive Summary	1
1. Measurement of Rock Properties	4
1.1. Caprock Integrity Laboratory	4
1.2. Measurement of Permeability by Pressure-Pulse Decay	10
1.3. Measurement of Permeability by Pressure-Pulse Decay with Digital Data Acquisition	12
1.4. Measurement of Permeability by Steady Flow	15
1.5. Correction of Steady Flow Measurements for Non-Ideality of Gases	18
1.6. Minimum Capillary Displacement Pressure and Effective Permeability	20
2. Proposal for Simultaneous Measurement of Axial and Radial Permeabilities from the Decay of a Pressure Pulse on the Entire Surface of a Core Plug	23
2.1. Fully-Immersed Pressure-Pulse Decay	23
2.2. Parameter Estimation Procedure and Sensitivity Analysis	26
3. Simulation of CO ₂ Migration and Trapping in Storage Reservoirs and Leakage through Seal Layers	28
3.1. Simulation of CO ₂ Injection into Middle Donovan Sands at Citronelle, Alabama, using TOUGHREACT	28
3.2. Effectiveness of Confining Layers: The Critical CO ₂ Column Height	38
3.3. Model for Leakage through a Seal Layer	41
4. Student Training	46
4.1. Student Training through Research	46
4.2. Student Training through Formal Course Work	48
5. Technology Transfer	50
Conclusion	55
Acronyms and Symbols	57
References	60

List of Tables

1.1.1. Measurements on rock samples in the Caprock Integrity Laboratory.	8
1.3.1. Conditions of the transient pressure-pulse test using nitrogen.	13
1.3.2. Conditions of the transient pressure-pulse test using helium.	14
1.4.1. Properties of Samples MSU2A and MSU2B.	16
2.1.1. Properties and experimental conditions for the simulation examples.	25
3.1.1. Primary input variables for the TOUGH2 simulations of carbon dioxide storage in Middle Donovan Sands.	29
3.1.2. Average initial volume fractions of primary mineral components identified in the sandstones of the Rodessa Formation in the Citronelle Oil Field.	29
3.1.3. Possible secondary minerals that could form during TOUGHREACT simulations of CO ₂ injection into the Middle Donovan.	30
3.3.1 Minimum capillary displacement pressure, maximum effective permeability, critical CO ₂ column height, and time to breakthrough for seal layers having absolute permeabilities of 0.5, 1, and 2 μdarcy.	42
4.2.1. The University of Alabama at Birmingham, Combustion Course Outline.	49

List of Figures

1.1.1.	The Caprock Integrity Laboratory at UAB.	4
1.1.2.	Early sample cell for measurements of permeability and minimum capillary displacement pressure.	5
1.1.3.	Early setup for measurement of permeability by steady flow.	6
1.1.4.	Current set up for measurement of the permeability of core sample plugs using the triaxial core holder with N ₂ or CO ₂ gas and measurement of the gas flow rate using a bubble film flow meter.	6
1.1.5.	Triaxial core holder in an oven, for measurements using supercritical CO ₂	7
1.2.1.	Time dependence of the dimensionless differential pressure across the sample.	10
1.3.1.	Setup of the cell shown in Figure 1.1.2 for measurements of permeability by pressure-pulse decay with digital data acquisition.	12
1.3.2.	Comparison of the series solution of Haskett et al. (1988) with transient pressure-pulse measurements for the Upper Pottsville Sandstone, using nitrogen.	13
1.3.3.	Comparison of the series solution of Haskett et al. (1988) with transient pressure-pulse measurements for the Upper Pottsville Sandstone, using helium.	14
1.4.1.	Upper Pottsville Sandstone Samples MSU2A and MSU2B.	15
1.4.2.	Measurements of permeability versus the reciprocal of the mean absolute pressure in the samples.	17
1.6.1.	Determination of the minimum capillary displacement pressure and effective permeability for the Boyles Sandstone sample.	22
2.1.1.	Conceptual schematic of a fully-immersed pressure-pulse-decay experiment.	23
2.1.2.	Effect of radial permeability on the pressure-pulse-decay experiment.	25
2.1.3.	Effect of axial permeability on the pressure-pulse-decay experiment.	26

List of Figures (continued)

2.2.1.	Example of the parameter-estimation procedure for the pressure-pulse-decay model. ..	27
2.2.2.	Correlation coefficient between the two principal permeabilities in the pressure-pulse-decay model.	27
3.1.1.	CO ₂ saturation at 100, 1000, and 10,000 years.	31
3.1.2.	Dissolved CO ₂ in the aqueous phase at 100, 1000, and 10,000 years.	31
3.1.3.	Siderite volume fractions at 100, 1000, and 10,000 years.	32
3.1.4.	Dawsonite volume fractions at 100, 1000, and 10,000 years.	33
3.1.5.	Ankerite volume fractions at 100, 1000, and 10,000 years.	33
3.1.6.	Calcite volume fractions at 100, 1000, and 10,000 years.	34
3.1.7.	Oligoclase volume fractions at 100, 1000, and 10,000 years.	34
3.1.8.	Quartz volume fractions at 100, 1000, and 10,000 years.	35
3.1.9.	Kaolinite volume fractions at 100, 1000, and 10,000 years.	35
3.1.10.	Porosity at 100, 1000, and 10,000 years.	36
3.1.11.	Permeability at 100, 1000, and 10,000 years.	37
3.1.12.	Cumulative CO ₂ mineralization at 100, 1000, and 10,000 years.	37
3.3.1.	Model calculations of CO ₂ leakage by capillary flow through seal layers as functions of permeability, thickness, and time.	44
3.3.2.	Evolution of a brine-saturated pore in a seal layer, in the presence of CO ₂	45

Executive Summary

The project entitled "Geologic Sequestration Training and Research," DOE Award Number DE-FE0002224, was performed by the University of Alabama at Birmingham and Southern Company from December 1, 2009, to June 30, 2013. As specified in the Funding Opportunity Announcement, DE-FOA-0000032 (June 29, 2009) from the National Energy Technology Laboratory, under which the project was awarded, the emphasis of the work was on training of students and faculty through research on topics central to further development, demonstration, and commercialization of carbon capture, utilization, and storage. The project had the following principal components: (1) establishment of a laboratory for the measurement of rock properties, able to accommodate special requirements, (2) evaluation of the sealing capacity of caprocks intended to serve as barriers to migration of CO₂ sequestered in geologic formations, (3) evaluation of the porosity, permeability, and storage capacity of reservoirs, (4) simulation of CO₂ migration and trapping in storage reservoirs and seepage through seal layers, (5) education and training of students through independent research on rock properties and reservoir simulation, and (6) development of an advanced undergraduate/graduate level course on coal combustion and gasification, climate change, and carbon sequestration.

The Caprock Integrity Laboratory, established under the present project, is fully functional and equipped for determination of porosity, absolute permeability, minimum capillary displacement pressure, and effective permeability to gas in the presence of brine, both for reservoir rocks having moderate to high permeability and for seal layers having low permeability. Measurements are made using a triaxial core holder, both by pressure-pulse decay and steady flow. Permeabilities in the microdarcy range, determined for identical samples by both methods, were in good agreement. The triaxial core holder is placed in an oven for experiments using supercritical CO₂.

Properties were determined for 19 rock samples provided by partners on other DOE/NETL projects. The sample having the lowest permeability, 0.28 ndarcy, was a roof rock from the Mary Lee coal seam in the Upper Pottsville Formation of Alabama, provided by the SECARB Phase II Black Warrior Basin Coal Seam Project. Two mudstones, having permeabilities of 2 ndarcy and 3 μ darcy, were provided by Advanced Resources International and the SECARB Phase III Anthropogenic CO₂ Injection Field Test, from confining layers in the Citronelle Dome in Southwest Alabama. Sixteen samples were sandstones provided by Southern Company for evaluation as possible candidates for biomineralization experiments in the Center for Biofilm Engineering at Montana State University, under the project entitled, "Advanced CO₂ Leakage Mitigation using Engineered Biomineralization Sealing Technologies." Three samples were practice, control, and biomineralized cores from that project, provided by Adrienne J. Phillips in the Center for Biofilm Engineering.

A model for CO₂ leakage through caprock, at pressures above the minimum capillary displacement pressure, was based on work by Hildenbrand and coworkers (2004), including a functional relationship between capillary pressure and the effective permeability to gas in the presence of a wetting phase. Under the conditions investigated, with a maximum CO₂ column

height of 54 m, doubling the absolute permeability of a 5-m-thick seal layer from 1 to 2 μ darcy, increased CO₂ loss by leakage over 100 years by a factor of five, from 0.8 to 4.1% of the CO₂ injected. Under the same conditions, no leakage by capillary flow was expected through a uniform seal having an absolute permeability of 0.5 μ darcy, in the absence of fractures.

Four graduate students and one undergraduate student conducted research in connection with this project, as described below. Two of the students have been awarded Ph.D. degrees for their work.

Richard A. Esposito, Principal Research Geologist with Southern Company and Senior/Key Co-Investigator on the present project, completed the requirements for the Ph.D. in Interdisciplinary Engineering, defended his dissertation, and graduated in December 2010. Dr. Esposito's dissertation is entitled: "Business models for commercial-scale carbon dioxide sequestration; with focus on storage capacity and enhanced oil recovery in Citronelle Dome." His dissertation includes: (1) assessments of the prospects for CO₂-enhanced oil recovery from the Citronelle Oil Field and the CO₂ storage capacity of saline formations in Citronelle Dome, a promising sequestration site in southwest Alabama, (2) analysis of the motivation and design for a CO₂-enhanced oil recovery and CO₂ storage pilot test in the Citronelle Oil Field, and (3) discussion of the business models that electric utility companies may choose to adopt for implementation of carbon capture and sequestration. Dr. Esposito is the first author of six refereed papers describing his and his coworkers' research on carbon capture, utilization, and storage.

Konstantinos Theodorou completed the requirements for the Ph.D. in Interdisciplinary Engineering, defended his dissertation, and graduated in August 2013. Dr. Theodorou's dissertation is entitled, "Carbon Dioxide Enhanced Oil Recovery from the Citronelle Oil Field and Carbon Sequestration in the Donovan Sand, Southwest Alabama." His research was focused on simulation, using the MASTER 3.0 reservoir simulator from NETL, of the CO₂-enhanced oil recovery pilot test conducted at Citronelle under a separate project, and on simulation of CO₂ injection and storage in the Middle Donovan saline formation in Citronelle Dome, using the TOUGH2-ECO2N and TOUGHREACT software suite from Lawrence Berkeley National Laboratory. In the latter work, 530,000 tonnes of CO₂ were injected through a single well into a formation 27.6 m thick at the rate of 36.3 t/day over 40 years. After 10,000 years, the CO₂ plume extends to a distance of 800 m from the injector and 50 kg of CO₂ per m³ of formation are sequestered in mineral phases, in a formation having an initial porosity of 13%. Of the formations in Citronelle Dome considered by Esposito et al. (2008) for CO₂ sequestration, none were found to have thickness exceeding the estimated critical height of CO₂ column that can be trapped under their shale caprocks indefinitely, without breakthrough. Dr. Theodorou is now an Instructor at Jefferson State Community College in Birmingham.

Michael J. Hannon, Jr., presented his research proposal and was admitted to candidacy for the Ph.D. in Interdisciplinary Engineering in May 2013. Mr. Hannon is working on the development of an alternative to traditional methods for measurement of the porosity and permeability of tight rocks, in which both axial and radial permeabilities could be determined simultaneously from transient pressure-pulse measurements on a cylindrical sample plug subjected to penetration by fluid at the same pressure on all of its surfaces. Mr. Hannon has succeeded in developing a numerical method for extraction of both axial and radial permeabilities from a hypothetical pressure trace. He assembled the apparatus for continuous digital data acquisition during traditional transient pressure-pulse measurements and wrote the

algorithm for determination of porosity and permeability from the record of upstream and downstream pressures. Mr. Hannon gave a poster presentation of his work, entitled "Sensitivity Analyses of a Fully Immersed Pressure-Pulse Decay Experiment on Cylindrical Samples of Layered Porous Media," at the Inverse Problems Symposium in Huntsville, AL, June 9-11, 2013.

Ph.D. student Kirk M. Ellison began work toward his Doctorate in Interdisciplinary Engineering at UAB in January 2012. Mr. Ellison is a Research Scientist at Southern Company, and received his Master's Degree in 2011 from the Department of Environmental Engineering and Earth Science at Clemson University, working with Professor Ronald W. Falta. Mr. Ellison is preparing his proposal for research on permanent storage of solid waste from coal-fired electric power generation and modeling and simulation of CO₂ storage in geologic formations, with validation using results from the large-scale demonstration of carbon capture, transportation, and geologic storage being conducted for SECARB by the Southern States Energy Board and their partners at Alabama Power Plant Barry and the Citronelle Oil Field, north of Mobile, AL.

Aaron D. Lamplugh, an undergraduate student in the Global and Community Leadership Honors Program, graduated from UAB with the degree of Bachelor of Science in Mechanical Engineering in May 2012. Mr. Lamplugh worked on the experimental measurement of rock properties, conducting measurements of the permeability of Bremen Sandstone and testing an apparatus for measurement of the permeability of tight rocks by steady flow. Mr. Lamplugh's poster presentation of his independent study project, "Sealing Capacity of Confining Layers," at UAB EXPO, the University's Annual Exposition of Undergraduate Scholarship, was awarded Third Place in April 2011 and the award for "Most Interesting Graphics on Poster" in the Engineering Competition Area. Mr. Lamplugh is now at the U.S. Department of Transportation John A. Volpe National Transportation Systems Center in Cambridge, MA, working on improvement of transportation safety.

A traditional advanced undergraduate/graduate course on coal combustion, offered by the Department of Mechanical Engineering every other year, was augmented, under the present project, by including climate change, coal gasification, and carbon sequestration among the topics covered. The expanded course was offered during the Fall semester in 2010 and 2012. A total of 49 students completed the course in those two years. It has become a popular advanced elective in the Department of Mechanical Engineering.

1. Measurement of Rock Properties

1.1. Caprock Integrity Laboratory

Peter M. Walsh
Department of Mechanical Engineering
UAB

Michael J. Hannon, Jr.
Interdisciplinary Engineering Program
UAB

Aaron D. Lamplugh
Global and Community Leadership Honors Program
UAB

A laboratory was established and equipped with support from the present project and from a companion project with Alabama Power Company and Southern Company, entitled "Geologic Carbon Sequestration: Caprock Integrity Laboratory." A photograph of the laboratory space in March 2010, at the beginning of the present project, and a recent view of the lab are shown in Figure 1.1.1.



Figure 1.1.1. The Caprock Integrity Laboratory at UAB. Left: the laboratory space in March 2010, at the beginning of the present project. Right: a recent view of the laboratory. With the exception of the tool chest, which has been in the Principal Investigator's laboratories for many years, and the computer and furniture, provided by the School of Engineering and Department of Mechanical Engineering, all of the equipment and supplies for the laboratory were purchased with funding from the present project and the companion project supported by the Alabama Power Company and Southern Company.

To get the project underway and begin providing useful data to our partners as quickly as possible, but not having the knowledge and experience needed to determine the specifications for a triaxial core holder having all of the features needed for the work that was planned, a simple sample cell, shown in Figure 1.1.2, was assembled from pipe and compression fittings. The pipe nipple at the center of the cell was bored through, to accept a sample plug, and the plug was sealed into the pipe nipple using epoxy cement (Sadler, Rahnama, and Whittle, 1992). This arrangement worked well, but it does have several disadvantages: (1) the sample was unavailable for other measurements, outside the cell, having been cemented in place, (2) no axial or radial overburden pressures could be applied to the sample, (3) the pressure difference that could be imposed across the sample was limited by the rock sample strength (not, in our experience, by the strength of the epoxy), and (4) the triaxial core holder is, in fact, much more convenient to use, for its ease of changing samples and obtaining leak-tight set-ups. The sample cell was set up for measurements of permeability as shown in Figure 1.1.3.

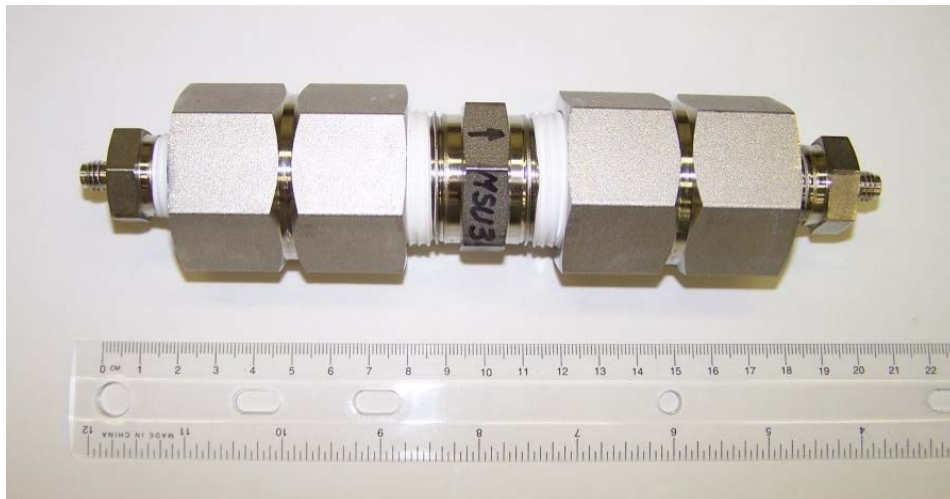


Figure 1.1.2. Early sample cell for measurements of permeability and minimum capillary displacement pressure. Core sample plugs 21 to 25 mm in diameter and 11 to 57 mm long were mounted in the 1-inch pipe nipple at the center, using epoxy cement (Sadler et al., 1992). The pipe nipple was bored out to accept the sample, with clearance for the cement.

After gaining experience through measurements using the cell shown in Figure 1.1.2, a triaxial core holder was designed to our specifications and fabricated by Core Lab/TEMCO. The triaxial core holder is now the equipment of choice for measurements of permeability and determination of minimum capillary displacement pressures. The setup for measurement of permeability by steady flow is shown in Figure 1.1.4. The flow rate and pressure drop across high permeability samples are controlled using a metering valve at the outlet from the core holder. The flow rate of gas through the sample is measured by timing the displacement of a soap film in a graduated tube (Teledyne Hastings Mini-Flo Calibrator, Model HBM-1A).



Figure 1.1.3. Early setup for measurement of permeability by steady flow. The sample cell shown in Figure 1.1.2 is in the lab clamp below and to the right of center in this photo. The flow rate of nitrogen gas through the core plug was measured by timing the displacement of water from the inverted burette or a graduated cylinder at higher gas flow rates. Slight reconfiguration of the plumbing enabled measurements by pressure-pulse decay.

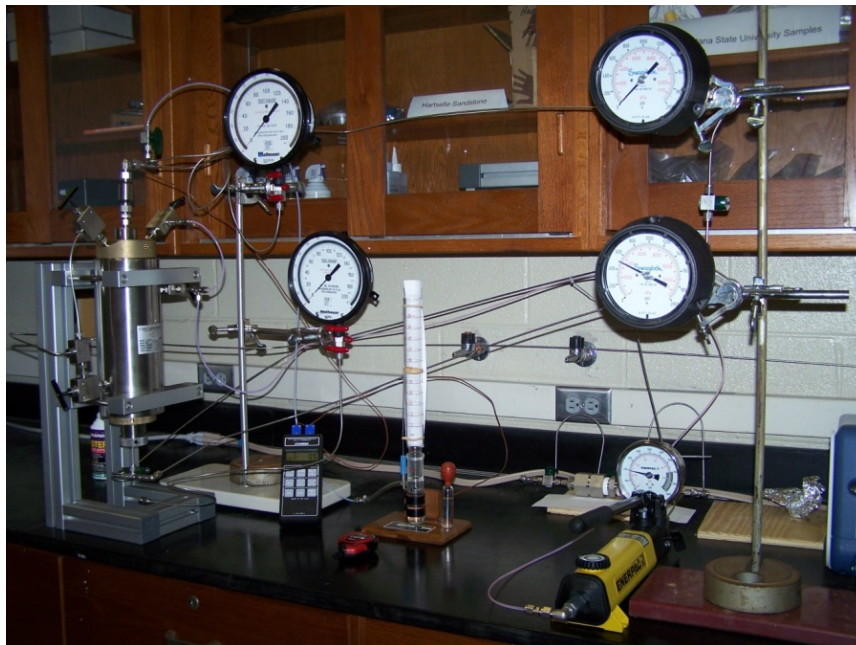


Figure 1.1.4. Current set up for measurement of the permeability of core sample plugs using the triaxial core holder with N_2 or CO_2 gas and measurement of the gas flow rate using a bubble film flow meter.

The triaxial core holder is placed in an oven, as shown in Figure 1.1.5, for experiments using supercritical CO₂.

Measurements that have been made, to date, on samples of reservoir rock and caprock are listed in Table 1.1.1. The measurements on the first page of the table were made using cells of the type shown in Figure 1.1.2. Measurements using the triaxial core holder are on the second page, beginning with the sandstone Practice Sample, No. T5, from Montana State University.

Samples have been provided by Advanced Resources International, Geological Survey of Alabama, Montana State University, Southeast Regional Carbon Sequestration Partnership (SECARB), and Southern Company. Some examples of the measurements that have been made are described in the following sections.



Figure 1.1.5. Triaxial core holder in an oven, for measurements using supercritical CO₂.

Table 1.1.1. Measurements on rock samples in the Caprock Integrity Laboratory.

Rock	Source	ID	Sample	Orientation	Measurement	Fluid	Value	Method
Shale	Black Warrior Basin, AL	BW No. 2	22 mm diameter, 11 mm-long plug	Perpendicular ^a	Porosity Permeability	water ^c N ₂	3.6% 0.28 ndarcy	Imbibition Pressure-pulse decay
Pottsville 1377.5 ft	Mary Lee coal zone Roof rock, SECARB							
Sandstone	Boyles Sandstone Pottsville Formation, Etowah County, AL Southern Company	S2-H-Plug	22 mm diameter 54 mm-long plug	Parallel ^a	Porosity Permeability Permeability Minimum capillary displacement press. ^d	water ^c N ₂ N ₂ water, ^c N ₂	8.69% 0.42 mdarcy 0.46 mdarcy 10 psi	Imbibition Steady flow Pressure-pulse decay Pressure-pulse decay
Sandstone	Upper Pottsville Fishtrap Mine AL Power Plant Miller	MSU2A	22 mm diameter 57 mm-long plug	Perpendicular ^a	Porosity Permeability Permeability Permeability	water ^b N ₂ N ₂ He	3.84% 1.55 μdarcy 1.42 μdarcy 1.58 μdarcy	Imbibition Steady flow Pressure-pulse decay Pressure-pulse decay
Sandstone	Upper Pottsville Fishtrap Mine AL Power Plant Miller	MSU2B	21 mm diameter 56 mm-long plug	Perpendicular ^a	Porosity Permeability	water ^c N ₂	3.64% 1.45 μdarcy	Imbibition Steady flow
Sandstone	Bremen Sandstone AL Power Co., Lewis Smith Dam	MSU3	21.5 mm diameter 54.5 mm-long plug	Parallel ^a	Porosity Permeability	water ^c N ₂	13.79% 31.6 mdarcy	Imbibition Steady flow
Sandstone	Hartselle Sandstone Jefferson County, AL Southern Company	#1 Parallel I	21.2 mm diameter 49.4 mm-long plug	Parallel ^a	Porosity Permeability	water ^c N ₂	9.15% 19.5 mdarcy	Imbibition Steady flow
Sandstone	Hartselle Sandstone Morgan County, AL Southern Company	#2 Parallel I	24.4 mm diameter 54.0 mm-long plug	Parallel ^a	Porosity Permeability	water ^c N ₂	9.89% 5.0 mdarcy	Imbibition Steady flow
Sandstone	Hartselle Sandstone Morgan County, AL Southern Company	#3 Parallel I	21.7 mm diameter 56.2 mm-long plug	Parallel ^a	Porosity Permeability	water ^c N ₂	7.19% < 0.1 μdarcy	Imbibition Steady flow
Sandstone	Bremen Sandstone Montana State University	1206 H4	24.8 mm diameter 50.9 mm-long plug	Parallel ^b	Porosity Permeability	water ^c N ₂	11.6% 8.5 mdarcy	Imbibition Steady flow
Sandstone	Bremen Sandstone Montana State University	1206 V2	25.0 mm diameter 51.0 mm-long plug	Perpendicular ^b	Porosity Permeability	water ^c N ₂	12.2% 1.7 mdarcy	Imbibition Steady flow

Please see the notes at the end of the table, on the following page.

Table 1.1.1 (continued). Measurements on rock samples in the Caprock Integrity Laboratory.

Rock	Source	ID	Sample	Orientation	Measurement	Fluid	Value	Method
Sandstone	Practice Montana State University	T5	25.0 mm diameter 51.4 mm-long plug	e	Permeability	CO ₂ gas	81 mdarcy	Steady flow
Sandstone	Control Montana State University A. J. Phillips (2013)	NT8	24.9 mm diameter 50.6 mm-long plug	e	Permeability Minimum capillary displacement press. ^d	CO ₂ gas brine, ^f N ₂	71.6 mdarcy 0.1 ^g psid	Steady flow Pressure-pulse decay
Sandstone	Biom mineralized Montana State University A. J. Phillips (2013)	NT9	25.0 mm diameter 51.2 mm-long plug	e	Permeability Minimum capillary displacement press. ^d	CO ₂ gas brine, ^f N ₂	3.27 mdarcy 3.7 psid	Steady flow Pressure-pulse decay
Undifferentiated Sandstone Upper Pottsville	Brookwood, AL Carter Coal Seam Southern Company	CS #2	24.7 mm diameter 51.0 mm-long plug	h	Permeability	CO ₂ gas	1.014 μdarcy	Steady flow
Undifferentiated Sandstone Upper Pottsville	Brookwood, AL Carter Coal Seam Southern Company	CS #3	24.7 mm diameter 51.0 mm-long plug	h	Permeability	CO ₂ gas	0.31 μdarcy	Steady flow
Boyles Sandstone Unweathered	Duck River Dam N of Cullman, AL Southern Company	LS-1	25.05 mm diameter 44.5 mm-long plug	Parallel ^a	Permeability	CO ₂ gas	0.0345 mdarcy	Steady flow
Boyles Sandstone Weathered	Duck River Dam N of Cullman, AL Southern Company	LS-2 (long)	25.05 mm diameter 38.5 mm-long plug	~ 45° ^a	Permeability	CO ₂ gas	0.1282 mdarcy	Steady flow
Mudstone Upper Paluxy 9431.3 ft	Citronelle SE Unit Well D-9-9 No. 2 Advanced Resources Int'l	2FD	25.2 mm diameter 26.8 mm-long plug	Perpendicular ^a	Permeability	CO ₂ gas	2.95 μdarcy	Steady flow
Mudstone Upper Paluxy 9442.1 ft	Citronelle SE Unit Well D-9-9 No. 2 Advanced Resources Int'l	3FD	24.6 mm diameter 26.4 mm-long plug	Perpendicular ^a	Permeability	N ₂	2 ndarcy	Steady flow

a. Relative to bedding plane.
b. Relative to ground surface.
c. Distilled.

d. Hildenbrand et al. (2002, 2004).
e. Not available
f. 10 g NaCl/L

g. Approximately equal to the hydrostatic head.
h. Unknown

1.2. Measurement of Permeability by Pressure-Pulse Decay

Peter M. Walsh
 Department of Mechanical Engineering
 UAB

The determination of the permeability of the first sample listed in Table 1.1.1 is presented here as an example. The sample, provided by Jack C. Pashin at the Geological Survey of Alabama, from the Upper Pottsville core collected by the SECARB Phase II Black Warrior Basin Coal Seam Project, is a 7/8-inch diameter plug of core from Monitor Well 3N, identified as roof rock from the Mary Lee coal zone at 1377.5 feet. The axis of the sample is perpendicular to the bedding plane. The porosity of the sample, determined by imbibition of distilled water, is 3.6%.

Permeability was determined by the pressure-pulse decay method, using nitrogen. The record of pressure decay (differential pressure/initial differential pressure) is shown in Figure 1.2.1.

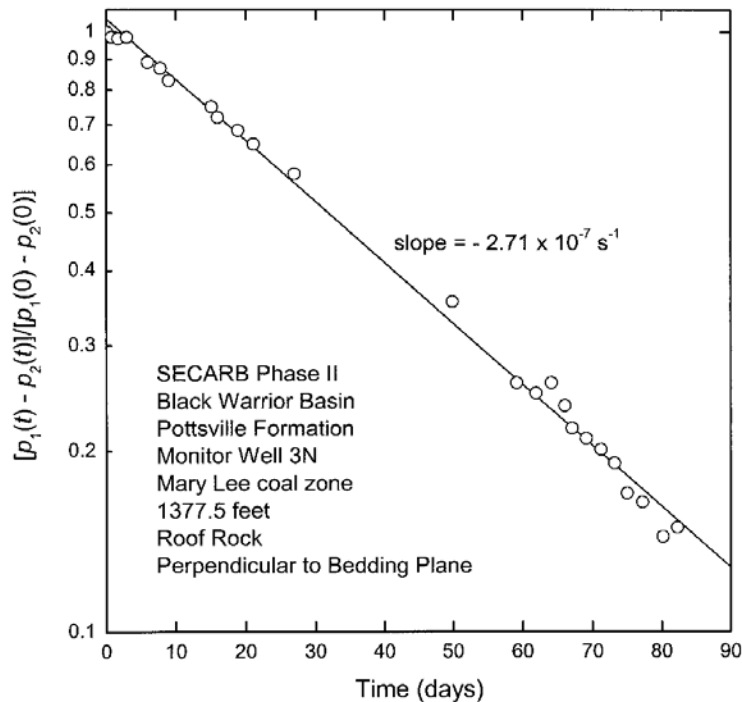


Figure 1.2.1. Time dependence of the dimensionless differential pressure across the sample. The initial upstream and downstream pressures were 1101 and 1001 psig, respectively.

The pressure decay is given by the following equation, when the pore volume in the rock sample is smaller than the volumes of the upstream and downstream cavities in the sample holder (Dicker and Smits, 1988):

$$\frac{p_1 - p_2}{p_{1,0} - p_{2,0}} = \exp\left(-\frac{k f(a,b)}{c \mu \phi L^2} t\right) \quad (1.2.1)$$

where:

$$f(a,b) = (a + b + ab) - \frac{1}{3}(a + b + 0.4132 ab)^2 + 0.0744 (a + b + 0.0578 ab)^3 \quad (1.2.2)$$

and

a	ratio of pore volume in the specimen to the upstream chamber volume, $\phi V/V_1$, = 0.00556, dimensionless
b	ratio of pore volume in the specimen to the downstream chamber volume, $\phi V/V_2$, = 0.00560, dimensionless
c	isothermal compressibility of N ₂ , = 0.1346 x 10 ⁻⁶ Pa ⁻¹ (Lemmon et al., 2007)
$f(a,b)$	function defined by Equation (1.2.2), = 0.01115, dimensionless
k	permeability, m ²
L	length of the specimen, = 0.01113 m
p_1	instantaneous absolute pressure in the upstream chamber, Pa
$p_{1,0}$	initial absolute pressure in the upstream chamber, = 7.692 x 10 ⁶ Pa
p_2	instantaneous absolute pressure in the downstream chamber, Pa
$p_{2,0}$	initial absolute pressure in the downstream chamber, = 7.003 x 10 ⁶ Pa
s	slope of the line in the plot of the logarithm of dimensionless pressure versus time, = - 2.71 x 10 ⁻⁷ s ⁻¹
t	time, s
V	bulk volume of the specimen, = 4.094 x 10 ⁻⁶ m ³
V_1	volume of the upstream chamber, = 26.44 x 10 ⁻⁶ m ³
V_2	volume of the downstream chamber, = 26.24 x 10 ⁻⁶ m ³
μ	absolute viscosity of N ₂ at the temperature and mean pressure of the test (Lemmon et al., 2007), = 19.046 x 10 ⁻⁶ Pa·s
ϕ	porosity of the specimen, = 0.036, dimensionless

The slope of the line on the semi-log plot in Figure 1.2.1 is the coefficient of time in the exponent in Equation (1.2.1). Rearranging, to find the permeability in terms of the experimentally determined slope, s , gives:

$$k = - \frac{c \mu \phi L^2 s}{f(a,b)} \quad (1.2.3)$$

Substitution of the values in Equation (1.2.3) gives an absolute permeability for the shale sample,

$$k = (2.77 \pm 0.10) \times 10^{-22} \text{ m}^2 = 0.28 \pm 0.01 \text{ ndarcy.}$$

The uncertainty is based upon the range of slopes that could reasonably be fit to the measurements in Figure 1.2.1.

1.3. Measurement of Permeability by Pressure-Pulse Decay with Digital Data Acquisition

Michael J. Hannon, Jr.
Interdisciplinary Engineering Program
UAB

Early work on the development of the transient pressure-pulse measurement technique was reported by Brace et al. (1968). Hsieh et al. (1981) solved the governing partial differential equation, combining the differential form of Darcy's Law with the continuity equation for liquid as the permeating fluid, and performing the analysis using Laplace transforms, based on the methods of Carslaw and Jaeger (1959) for heat conduction in solids. Haskett et al. (1988) modified the Navier-Stokes equations for gas flow through porous media to fit a similar form, following the solution technique of Hsieh et al. (1981). The evolution of the mathematical model is described by Ning (1992).

The permeability of a sandstone sample was measured using the pressure-pulse decay technique with digital data acquisition. The sample is the third in the list in Table 1.1.1, from the Upper Pottsville Formation, collected by Richard Esposito at the Fishtrap Mine, a quarry near Alabama Power Co.'s Plant Miller. This sandstone was under consideration for biomineralization experiments in the Center for Biofilm Engineering at Montana State University, under a separate project (Phillips, 2013).* The tests were performed using the equipment shown in Figure 1.3.1, with both nitrogen and helium as fluid.

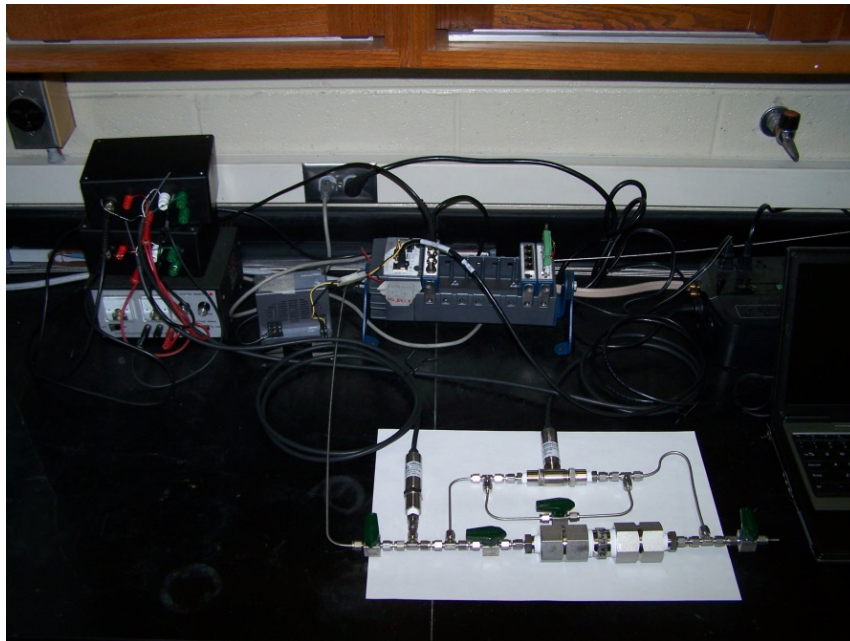


Figure 1.3.1. Setup of the cell shown in Figure 1.1.2 for measurements of permeability by pressure-pulse decay with digital data acquisition.

*Award Number DE-FE0004478 to Montana State University from the National Energy Technology Laboratory, entitled: "Advanced CO₂ Leakage Mitigation using Engineered Biomineralization Sealing Technologies."

Tables 1.3.1 and 1.3.2 give the conditions of the measurements using nitrogen and helium, respectively. The porosity of the sample could not be determined in conjunction with the permeability using the transient technique, because the upstream and downstream reservoir volumes were too large, so the porosity measured by imbibition, 3.84%, was specified as an input to the data analysis scheme. Values for the absolute permeability were determined by a least-squares fit of the series solution of Haskett et al. (1988) to the measurements. Comparison of the optimum solutions with the measurements using nitrogen and helium are shown in Figures 1.3.2 and 1.3.3, respectively. The values determined using both nitrogen (1.42 μ darcy) and helium (1.58 μ darcy) are in good agreement with the permeability determined by steady flow of nitrogen (1.55 μ darcy), presented in the following section.

Table 1.3.1. Conditions of the transient pressure-pulse test using nitrogen.

Condition	Value
Upstream reservoir volume	13.745 mL
Downstream reservoir volume	22.1339 mL
Sample length	56.50 mm
Sample diameter	21.54 mm
Temperature	75 °F
Initial pore pressure	997 psia
Pulse pressure	78 psid
Permeating fluid	N ₂

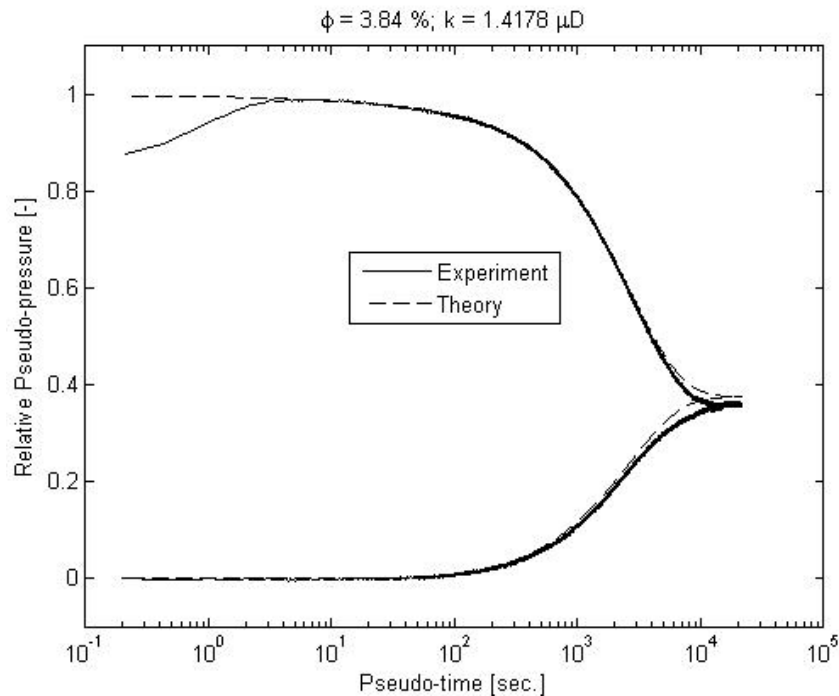


Figure 1.3.2. Comparison of the series solution of Haskett et al. (1988) with transient pressure-pulse measurements for the Upper Pottsville Sandstone, using nitrogen.

Table 1.3.2. Conditions of the transient pressure-pulse test using helium.

Condition	Value
Upstream reservoir volume	13.745 mL
Downstream reservoir volume	22.1339 mL
Sample length	56.50 mm
Sample diameter	21.54 mm
Temperature	75 °F
Initial pore pressure	1003 psia
Pulse pressure	51 psid
Permeating fluid	He

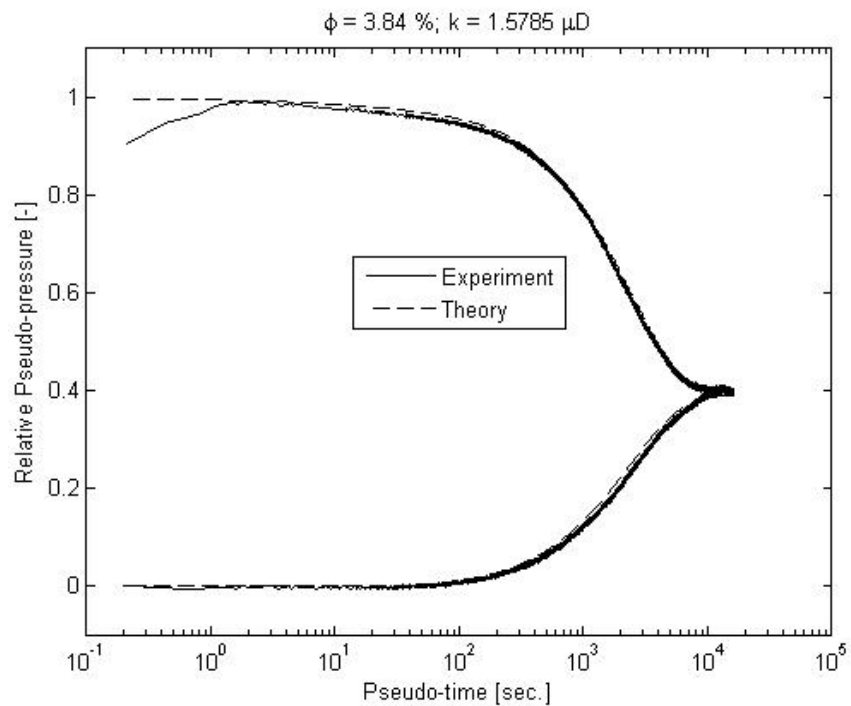


Figure 1.3.3. Comparison of the series solution of Haskett et al. (1988) with transient pressure-pulse measurements for the Upper Pottsville Sandstone, using helium.

1.4. Measurement of Permeability by Steady Flow

Peter M. Walsh
Department of Mechanical Engineering
UAB

Permeabilities of reservoir rocks having moderate to high permeability have been measured by steady flow of N_2 or CO_2 at room temperature. Measurements are made over a range of pressures at the entrance to the sample, at the highest pressures at which the flow rate can be measured with good reproducibility. At least four measurements of the flow rate are made at each pressure. The average effective permeability and standard deviation of the measurements at each pressure are plotted versus the reciprocal of the absolute pressure and extrapolated to high pressure to obtain the absolute permeability, corrected for slip (Klinkenberg, 1941; Collins, 1961; API, 1998; ASTM, 2008). Correction for non-ideality of the gas, especially important for CO_2 , is described in the following section.

Measurements of the permeabilities of the third and fourth samples listed in Table 1.1.1 are presented here as examples. The samples are $\frac{7}{8}$ -inch-in-diameter by $2\frac{1}{4}$ -inch-long sandstone plugs from the Upper Pottsville Formation, collected by Richard Esposito at the Fishtrap Mine, a quarry near Alabama Power Co.'s Plant Miller. The samples, labeled MSU2A and MSU2B are shown in Figure 1.4.1. Both have their axes perpendicular to the bedding plane.



Figure 1.4.1. Upper Pottsville Sandstone Samples MSU2A (top) and MSU2B (bottom).

Porosity and solid density of the samples, determined by the imbibition method using distilled water, are given in Table 1.4.1.

Table 1.4.1. Properties of Samples MSU2A and MSU2B.

Property	Symbol	Sample MSU2A	Sample MSU2B
Cross section area	A	$3.644 \times 10^{-4} \text{ m}^2$	$3.601 \times 10^{-4} \text{ m}^2$
Length	L	0.05651 m	0.05553 m
Permeability	k	$(1.53 \pm 0.05) \times 10^{-18} \text{ m}^2$ $1.55 \pm 0.05 \text{ \mu darcy}$	$(1.43 \pm 0.09) \times 10^{-18} \text{ m}^2$ $1.45 \pm 0.09 \text{ \mu darcy}$
Porosity	ϕ	3.84%	3.64%
Solid Density		2.72 g/cm^3	2.68 g/cm^3

Permeability was determined by measuring pressures and flow rates during steady flow of nitrogen through the samples at room temperature (22-24 °C). The setup for the measurements is shown in Figure 1.1.3. The sample plugs were mounted in 1-inch pipe nipples using epoxy cement, as described in Section 1.1. The upstream side of the sample holder was connected to high-pressure nitrogen, with the other side open to the atmosphere. The flow rate of gas through the sample was determined by timing the displacement of water from an inverted burette by the gas leaving the sample holder. In this setup no confining stress was imposed on the sample.

Permeability was determined at four or five pressures at the inlet to the sample over the range from 26 to 197 psig (0.28 to 1.46 MPa, absolute). The permeability at each pressure was calculated using the following equation (ASTM, 2008):

$$k = \frac{2 Q_e P_e \mu L}{(P_i^2 - P_e^2) A} \quad (1.4.1)$$

where:

- A cross-section area of the sample, m^2
- k coefficient of permeability, m^2
- L length of the sample, m
- P_e absolute pressure of gas at the exit from the sample, = barometric pressure, Pa
- P_i absolute pressure of gas at the inlet to the sample, Pa
- Q_e volumetric flow rate of gas at the exit from the sample, m^3/s
- μ absolute viscosity of nitrogen at the temperature and mean pressure in the sample (Lemmon et al., 2007), Pa·s

Graphs of the measured apparent permeability versus the reciprocal of the mean absolute pressure, $[(P_i + P_e)/2]^{-1}$ (Klinkenberg, 1941; Collins, 1961; ASTM, 2008), are shown in Figure 1.4.2. The y-intercept of the line fit to the measurements, where the dependence on reciprocal pressure is approximately linear, gives the absolute permeability of the sample. The

uncertainty is the standard error in the value of the y-intercept, determined by the linear least squares fitting routine. The dimensions and permeabilities of the two samples are given in Table 1.4.1. The permeabilities, 1.45 and 1.55 μ darcy, differ by 7%.

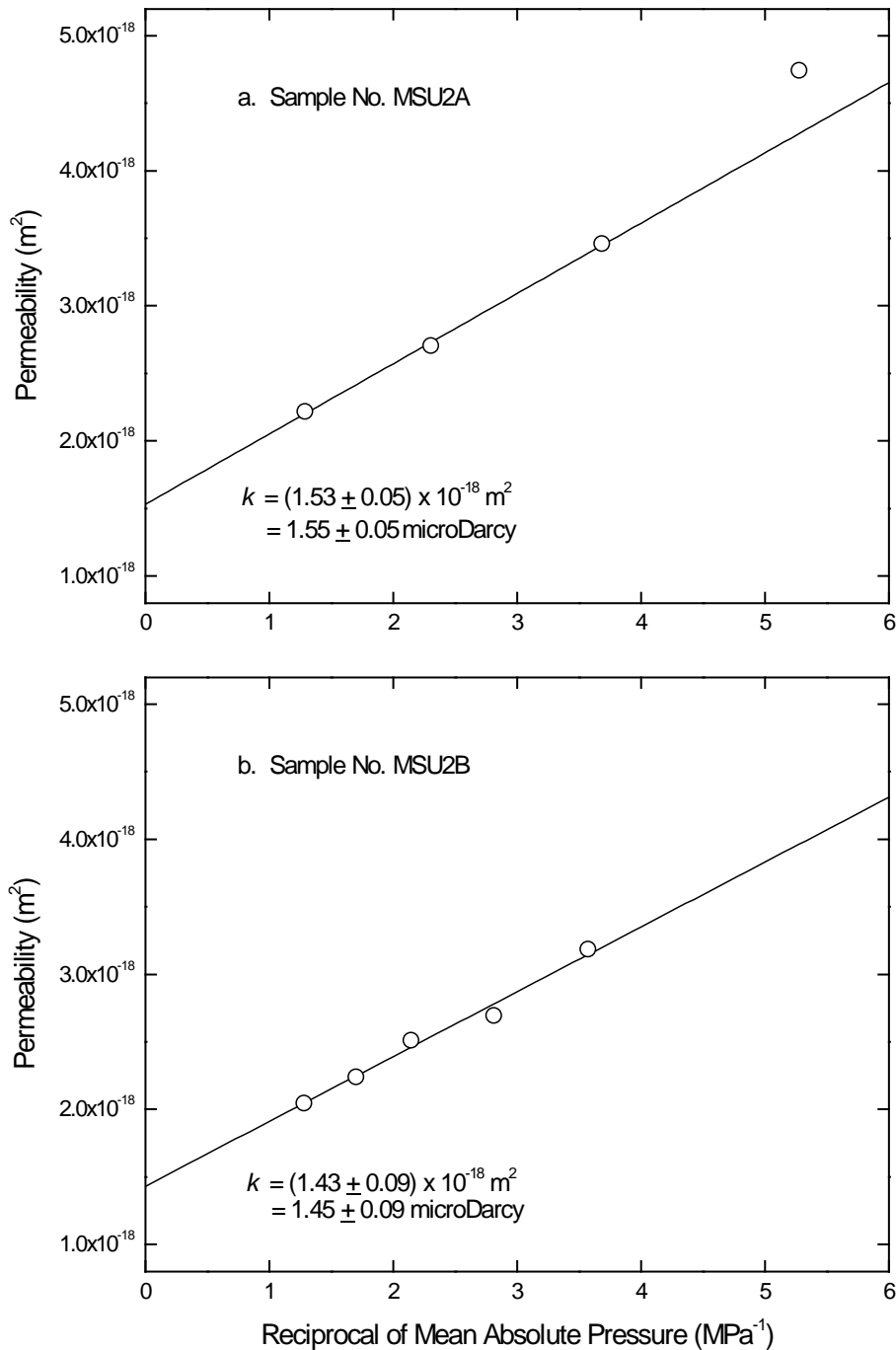


Figure 1.4.2. Measurements of permeability versus the reciprocal of the mean absolute pressure in the samples. Extrapolation to zero (high gas density), of the measurements in the region where the dependence on the reciprocal of mean pressure is approximately linear, corrects for "slip" (non-zero gas velocity at pore walls) at low gas density (Klinkenberg, 1941) and gives the absolute permeability of the rock, independent of the fluid.

1.5. Correction of Steady Flow Measurements for Non-Ideality of Gases

Peter M. Walsh
Department of Mechanical Engineering
UAB

Calculations of the effective permeability from measurements of steady flow of gas are often done using the following equation, obtained by integration of Darcy's law over the pressure difference from the inlet to the outlet from a core, assuming ideal behavior of the gas, i.e. that the product of pressure and the volumetric flow rate is constant at fixed temperature (ASTM, 2008). Please see Equation (1.4.1) on p. 16 for definitions of the symbols.

$$k = \frac{2 Q_e P_e \mu L}{(P_i^2 - P_e^2) A} \quad (1.5.1)$$

Under conditions typical of the measurements reported here, carbon dioxide deviates significantly from ideal gas behavior. For example, the density of CO₂, at 295 K and 200 psig is 28.891 kg/m³ (Lemmon et al., 2007), but the density according to the ideal gas law is 26.561 kg/m³, a difference of 8%.

An approximate correction for non-ideal gas behavior can be made by multiplying the right-hand side of Equation (1.5.1) by the ratio of the compressibility factor for the gas at the core temperature and mean pore pressure to the compressibility factor at the gas outlet conditions (API, 1998). This correction assumes that the compressibility factor is a constant, in the integration of Darcy's law over the pressure change from the inlet to the outlet of the core.

The following analysis accounts for continuous deviation of the *P-V-T* behavior of gases from the ideal gas law, over the length of the sample. The derivation begins with Darcy's law:

$$\frac{Q}{A} = - \frac{k dP}{\mu dx} \quad (1.5.2)$$

The assumption adopted to derive Equation (1.5.1) is that the product of pressure and the volumetric flow rate, *PQ*, is constant through the sample. Deviation from ideal gas behavior can be properly accounted for if the mass flow rate, *ṁ*, is assumed to be constant, instead:

$$\dot{m} = \rho Q = \text{constant} \quad (1.5.3)$$

Substituting Equation (1.5.3) into Darcy's law and rearranging:

$$\dot{m} dx = - \frac{k}{\mu} A \rho dP \quad (1.5.4)$$

The Virial equation of state for gases is (Sengers et al., 1972):

$$PV = NRT \left(1 + B_V \frac{P}{RT} + \dots \right) \quad (1.5.5)$$

Retaining only the first correction term and rearranging to obtain an expression for the density:

$$\rho = \frac{N W}{V} = \frac{P W}{R T} \frac{1}{1 + B_V \frac{P}{R T}} \quad (1.5.6)$$

The value of the second Virial coefficient, B_V , for carbon dioxide at 295 K is $-0.12605 \text{ m}^3/\text{kmol}$ (Lemmon et al., 2007), giving a density at 295 K and 200 psig of 28.7475 kg/m^3 , deviating by only 0.5% from the value for the density given by Lemmon et al. (2007).

Substituting the expression for gas density, Equation (1.5.6), into Equation (1.5.4), with boundary conditions, $P = P_i$ at $x = 0$ and $P = P_e$ at $x = L$:

$$\dot{m} \int_0^L dx = -A \frac{k}{\mu} \frac{W}{R T} \int_{P_i}^{P_e} \frac{P dP}{1 + B_V \frac{P}{R T}} \quad (1.5.7)$$

gives, after integration and rearrangement, the following expression for the permeability:

$$k = \frac{\frac{\dot{m}}{W} \frac{\mu L}{A}}{\frac{P_i - P_e}{B_V} - \frac{R T}{B_V^2} \ln \frac{1 + \frac{B_V P_i}{R T}}{1 + \frac{B_V P_e}{R T}}} \quad (1.5.8)$$

Equation (1.5.8) is used to determine the effective permeability from measurements of inlet and outlet pressures, the volumetric flow rate at ambient conditions, temperature in the core, the dimensions of the sample, the value for the second Virial coefficient of CO_2 or N_2 at the temperature in the core (Lemmon et al., 2007), the gas density at ambient conditions (at which the volumetric flow rate is measured), and the viscosity of the gas at the temperature and mean pressure in the core (Lemmon et al., 2007).

1.6. Minimum Capillary Displacement Pressure and Effective Permeability

Peter M. Walsh
Department of Mechanical Engineering
UAB

A drill core from the Boyles Sandstone Member of the Pottsville Formation in Etowah County, AL, was collected by Richard Esposito in February 2011. A 7/8-inch-diameter by 2-inch-long plug from the core, Sample No. S2-H-Plug, underwent a series of tests, including measurement of its minimum capillary displacement pressure and effective permeability, as described below.

Porosity, determined by the imbibition method using distilled water, was 8.7%. A measurement of the permeability of the sample by steady flow (ASTM, 2008), using nitrogen, with correction for the Klinkenberg effect (Klinkenberg, 1941; Collins, 1961) was $(4.18 \pm 0.20) \times 10^{-16} \text{ m}^2$ (0.42 ± 0.02 mdarcy). Two measurements of the permeability by pressure-pulse decay (Dicker and Smits, 1988) gave values of $4.57 \times 10^{-16} \text{ m}^2$ (0.46 mdarcy) and $4.81 \times 10^{-16} \text{ m}^2$ (0.49 mdarcy). The average of the three measurements is $(4.5 \pm 0.3) \times 10^{-16} \text{ m}^2$ (0.46 ± 0.04 mdarcy). These measurements were followed by determination of the minimum capillary displacement pressure and effective permeability.

The minimum capillary displacement pressure is the experimental result of the method developed by A. Hildenbrand and coworkers at RWTH in Aachen, Germany (Hildenbrand et al., 2002, 2004), for quantitative assessment of the potential for seepage of gas through fine-grained rocks. The set-up was similar to those used for the measurements of permeability. The sample was first saturated with water by mounting it vertically, then filling the upper, upstream cavity with water and applying a steady pressure of nitrogen until a few milliliters of water appeared on the downstream side. The cell was then inverted and excess water removed from the upstream cavity. Nitrogen at 200 psig, above the anticipated breakthrough pressure, was then applied to the upstream (now the lower) end of the plug, with the other end at atmospheric pressure, and the valves on both ends were closed.

As gas flows through the sample, the difference in pressure between the upstream and downstream cavities asymptotically approaches a residual pressure difference characteristic of the rock, corresponding to the capillary pressure in the narrowest throat in the highest conductivity pore connecting the upstream and downstream faces of the sample. This is the "minimum capillary displacement pressure," above which capillary flow of gas will occur through a rock initially saturated with the wetting phase, given sufficient time. The measurement is an alternative to the traditional method of increasing the pressure of gas on one face of a brine-saturated plug in small increments, until breakthrough is observed. The traditional method tends to overestimate the breakthrough pressure, because there can be a lag time of days or weeks before gas appears on the downstream side of a plug, even at upstream pressures well above the pressure ultimately identified as the breakthrough pressure.

The time dependence of the upstream and downstream pressures across the water-saturated plug is shown in Figure 1.6.1a. Just after the upstream and downstream cavities are sealed, at time = 0, the initial decay of the upstream pressure and rise in downstream pressure are

relatively slow because the water saturation of the rock is high. As water is displaced from the largest pores connecting the upstream and downstream faces, the permeability of the sample to the gas increases and the rates of the pressure changes increase, eventually passing through a maximum at the minimum water saturation reached under the conditions of the measurement. The instantaneous effective permeability is given by (Hildenbrand et al., 2002):

$$k_{eff} = - \frac{2 \mu L V_1}{A (p_1^2 - p_2^2)} \frac{\Delta p_1}{\Delta t} \quad (1.6.1)$$

where:

- A cross section area of the sample perpendicular to the flow direction, = $3.661 \times 10^{-4} \text{ m}^2$
- k_{eff} effective permeability to gas in the presence of a wetting phase, m^2
- L length of the specimen, = 0.05412 m
- p_1 instantaneous absolute pressure in the upstream chamber, Pa
- p_2 instantaneous absolute pressure in the downstream chamber, Pa
- V_1 volume of the upstream chamber, = $46.1 \times 10^{-6} \text{ m}^3$
- Δt time interval corresponding to the change in upstream pressure, Δp_1 , s
- μ absolute viscosity of N_2 at the temperature and mean pressure of the test (Lemmon et al., 2007), = $17.813 \times 10^{-6} \text{ Pa}\cdot\text{s}$

The dependence of the effective permeability on time is shown in Figure 1.6.1b. The maximum effective permeability, where the water saturation of the sample is lowest, under the conditions of the measurement, is $(0.433 \pm 0.006) \times 10^{-16} \text{ m}^2$ ($0.0439 \pm 0.0006 \text{ mDarcy}$), approximately 10% of the absolute permeability of the sandstone. After passing through the maximum effective permeability, as the pressure difference across the sample decreases further, water is reimbibed into the smallest of the gas-filled pores connecting the upstream and downstream faces of the sample. The process of reimbibition continues in successively larger pores, until the largest open pore connecting the upstream and downstream faces closes, cutting off capillary flow of gas through the sample. The remaining pressure difference, equal to the capillary pressure in the narrowest throat in the last pore to close, is the minimum capillary displacement pressure, equal to 0.07 MPa (10 psi), a relatively low value because the sandstone is closer to a reservoir rock than to a seal layer.

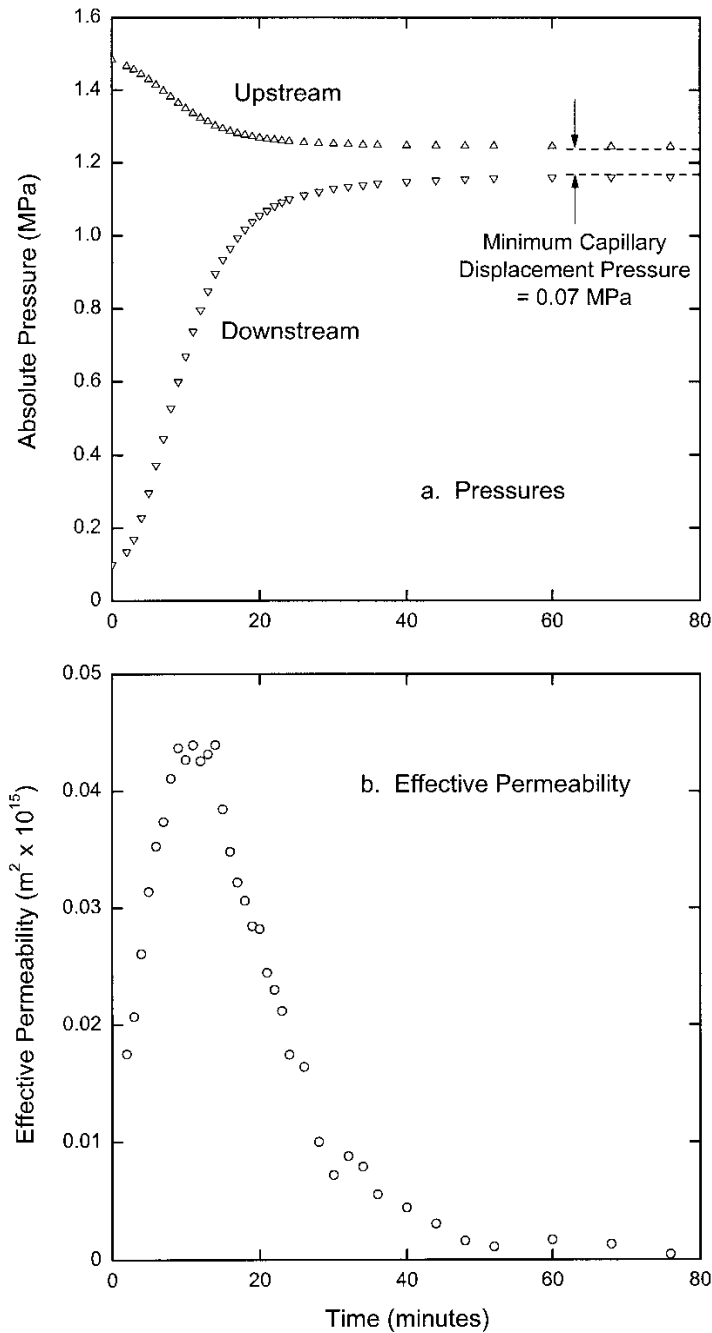


Figure 1.6.1. Determination of the minimum capillary displacement pressure and effective permeability for the Boyles Sandstone sample. a. Pressures in sealed cavities upstream and downstream from the sample versus time, starting at initial pressures of 215.1 and 14.5 psia, upstream and downstream, respectively. The minimum capillary displacement pressure is 10 psi. b. Effective permeability versus time, first increasing as water is displaced from the highest conductivity pores, increasing the gas saturation, and passing through a maximum at the lowest water saturation reached under the conditions of the measurement, then decreasing as water is reimbibed, first into the smallest of the open continuous pores and finally, at the minimum capillary displacement pressure, into the highest conductivity pore connecting the upstream and downstream faces of the sample.

2. Proposal for Simultaneous Measurement of Axial and Radial Permeabilities from the Decay of a Pressure Pulse on the Entire Surface of a Core Plug*

Michael J. Hannon, Jr.
Interdisciplinary Engineering Program
UAB

2.1. Fully-Immersed Pressure-Pulse Decay

The advent of permeametry and porosimetry measurements by pressure-pulse decay, using cylindrical core samples, arose from the need to more quickly characterize low-permeability geologic formations in the laboratory. However, due to time and leakage limitations, measurements on samples having ultra-low permeabilities, in the nanodarcy range or lower, are difficult using conventional pressure-pulse techniques. The present study is an enhancement of the pulse-decay technique in which the sample is fully immersed in the permeating fluid, as shown in Figure 2.1.1, exposing the entire outer surface of the sample to the pressure pulse. This arrangement has the potential to decrease test times by orders of magnitude. An additional benefit from this technique is the possibility for simultaneous measurement of the permeabilities parallel and perpendicular to the bedding plane of the formation from which the sample was cut.

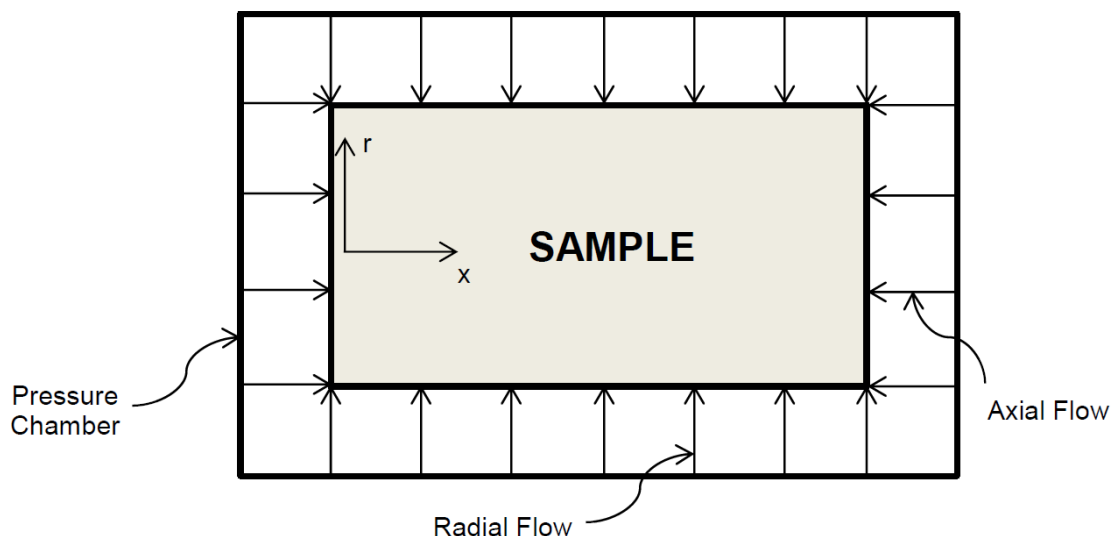


Figure 2.1.1. Conceptual schematic of a fully-immersed pressure-pulse-decay experiment.

*M. J. Hannon, Jr., "Sensitivity Analyses of a Fully Immersed Pressure-Pulse Decay Experiment on Cylindrical Samples of Layered Porous Media," Poster presentation at the 2013 Inverse Problems Symposium, Huntsville, AL, June 9-11, 2013.

A cylindrical sample of length L , radius R , and porosity ϕ is placed in a reservoir of volume V_r . The internal pore pressure p in the sample, as well as the pressure in the surrounding reservoir, p_r , are equilibrated to an initial pressure p_0 . The reservoir pressure is then instantaneously increased to a slightly higher (typically by 5 to 10%) level p_p . Assuming the permeabilities in the axial (x) and radial (r) directions to be the primary axes of permeability, having principal values k_x and k_r , respectively, the pressure-decay behavior, following the instantaneous step change in pressure, is modeled by Equations (2.1.1) to (2.1.5):

$$\phi \frac{\partial}{\partial t} \left(\frac{p}{z} \right) = k_r \frac{1}{r} \frac{\partial}{\partial r} \left(r \frac{p}{\mu z} \frac{\partial p}{\partial r} \right) + k_x \frac{\partial}{\partial x} \left(\frac{p}{\mu z} \frac{\partial p}{\partial x} \right) \quad (2.1.1)$$

$$p(r, x, t = 0) = p_0; \quad p_r(t = 0) = p_p \quad (2.1.2)$$

$$p(r = R, x, t) = p_r(t); \quad \frac{\partial p}{\partial r}(r = 0, x, t) = 0 \quad (2.1.3)$$

$$p(r, x = 0, t) = p_r(t); \quad \frac{\partial p}{\partial x}(r, x = L/2, t) = 0 \quad (2.1.4)$$

$$\frac{V_r}{z_r} \left(1 - \frac{p_r}{z_r} \frac{dz_r}{dp_r} \right) \frac{dp_r}{dt} = 4\pi \frac{p_r}{\mu_r z_r} \left[k_r R \int_0^{L/2} \frac{\partial p}{\partial r} \Big|_{r=R} dx - k_x \int_0^R \frac{\partial p}{\partial x} \Big|_{x=0} r dr \right] \quad (2.1.5)$$

The pressure response also depends on the dynamic viscosity μ and compressibility factor z of the gas in the pores and those of the gas in the reservoir surrounding the sample, μ_r and z_r , which, assuming an isothermal process, are functions of pressure. The properties and conditions specified in the simulations are given in Table 2.1.1. Using an explicit finite-difference numerical scheme accurate to first-order in time and accurate to second-order in space, the calculated reservoir pressure is shown versus time t for various values of k_r and k_x in Figures 2.1.2 and 2.1.3, respectively. These simulation examples are for permeabilities in the nanodarcy and sub-nanodarcy ranges, characteristic of layered caprock formations, such as shales.

Table 2.1.1.
Properties and experimental conditions
for the simulation examples.

Property	Value
Core porosity, ϕ	3.84%
Core length, L	1.00 in.
Core diameter, D	1.00 in.
Core volume, V_B	12.87 mL
Temperature, T	75 °F
Initial pressure, p_0	1000 psia
Pulse pressure, p_p	1050 psia
Permeating fluid	He

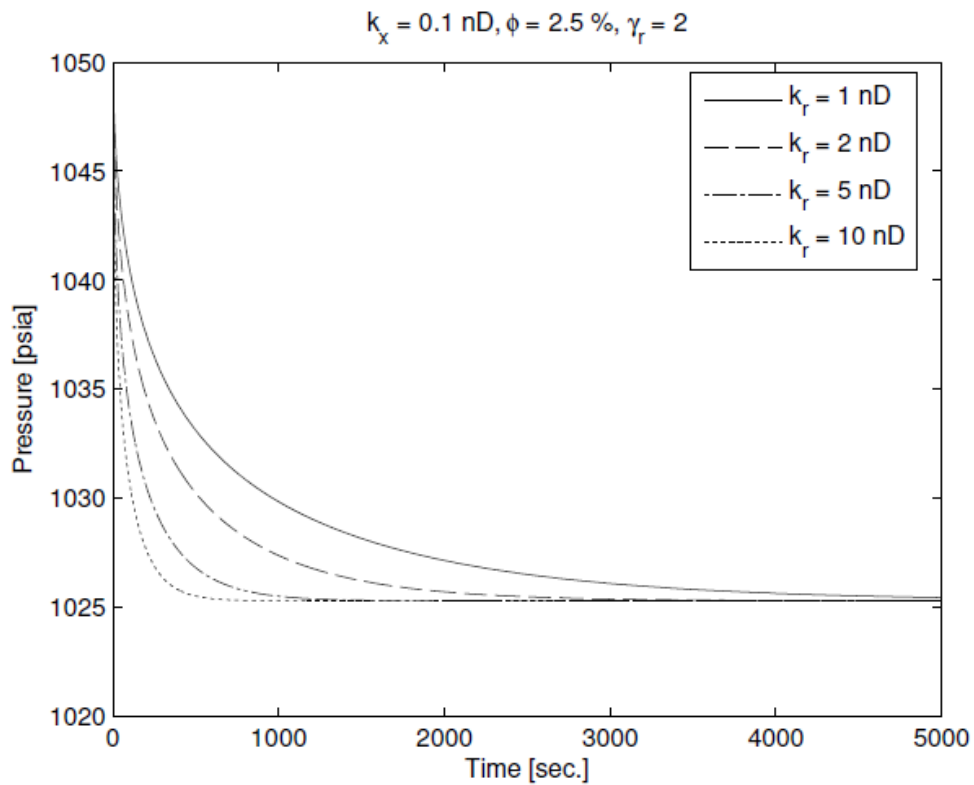


Figure 2.1.2. Effect of radial permeability on the pressure-pulse-decay experiment.

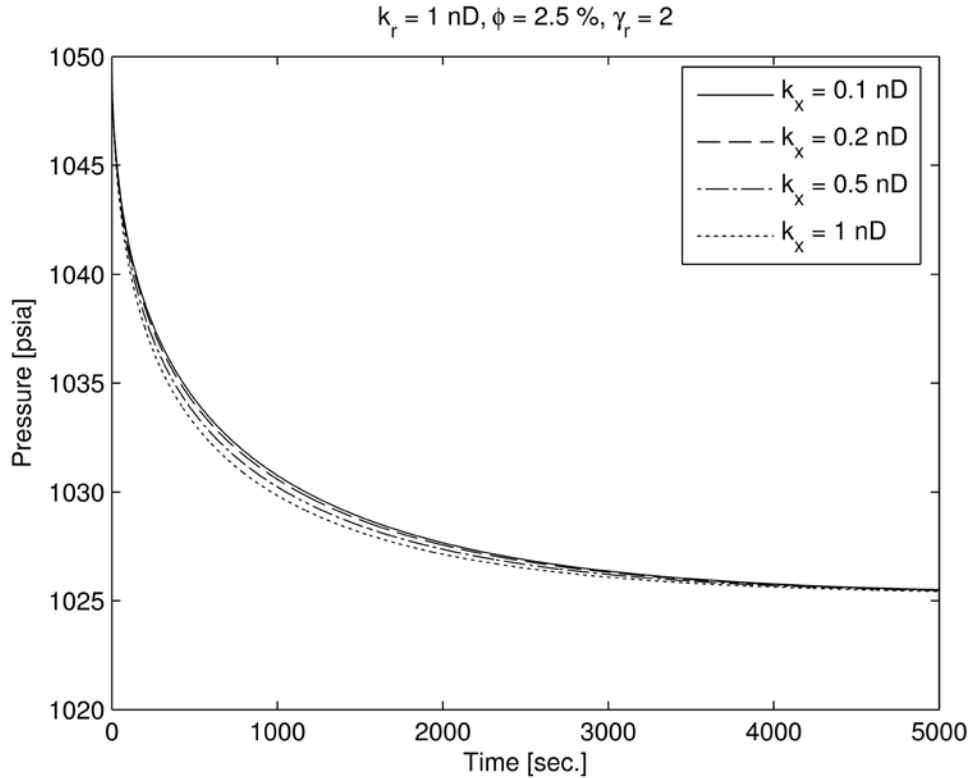


Figure 2.1.3. Effect of axial permeability on the pressure-pulse-decay experiment.

2.2. Parameter Estimation Procedure and Sensitivity Analysis

By comparing experimental records of the reservoir pressure to simulation output, one could simultaneously estimate k_x , k_r , and ϕ by minimizing the error using a Gauss method. Toward that end, a rough Monte Carlo analysis was performed to approximate experimental data by superimposing a normally-distributed error, based on the expected accuracy of the pressure measurements, on the simulation output. Following the inversion procedures described by Finsterle and Persoff (1997), the sensitivity coefficient matrix \mathbf{X} used in the Gauss method is based on the logarithm of the parameters rather than the parameters themselves. The final simulation time t_n is calculated to maximize the factor $\Delta^n \equiv \|\mathbf{X}^T \mathbf{X}\| / n^m$, as defined by Beck and Arnold (1977), where n is the number of data points and m the number of parameters. Based on a rough initial guess for the three parameters of interest, an example of the result of the parameter-estimation procedure is shown in Figure 2.2.1. In this case, an accurate estimate of the solution was found after 9 iterations, but the success of this procedure highly depends on the accuracy of the initial guess. From Figure 2.1.3, one sees that the model output is rather insensitive to k_x . As a result, the estimate of k_x (0.185 ndarcy vs. 0.2 ndarcy) is not as accurate as those of k_r (1.006 ndarcy vs. 1 ndarcy) and ϕ (3.839% vs. 3.84%). The insensitivity to k_x is somewhat mitigated at lower anisotropy ratios, k_r/k_x . However, this must be balanced by the fact that the correlation coefficient between k_r and k_x approaches -1 at short experimental times, as k_x approaches k_r , as shown in Figure 2.2.2.

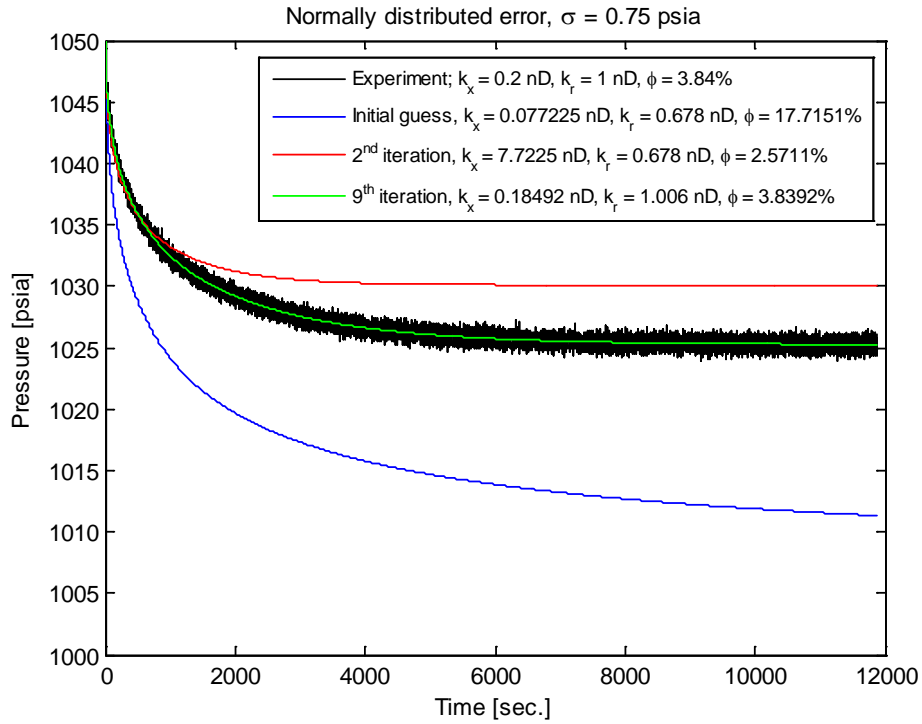


Figure 2.2.1. Example of the parameter-estimation procedure for the pressure-pulse-decay model.

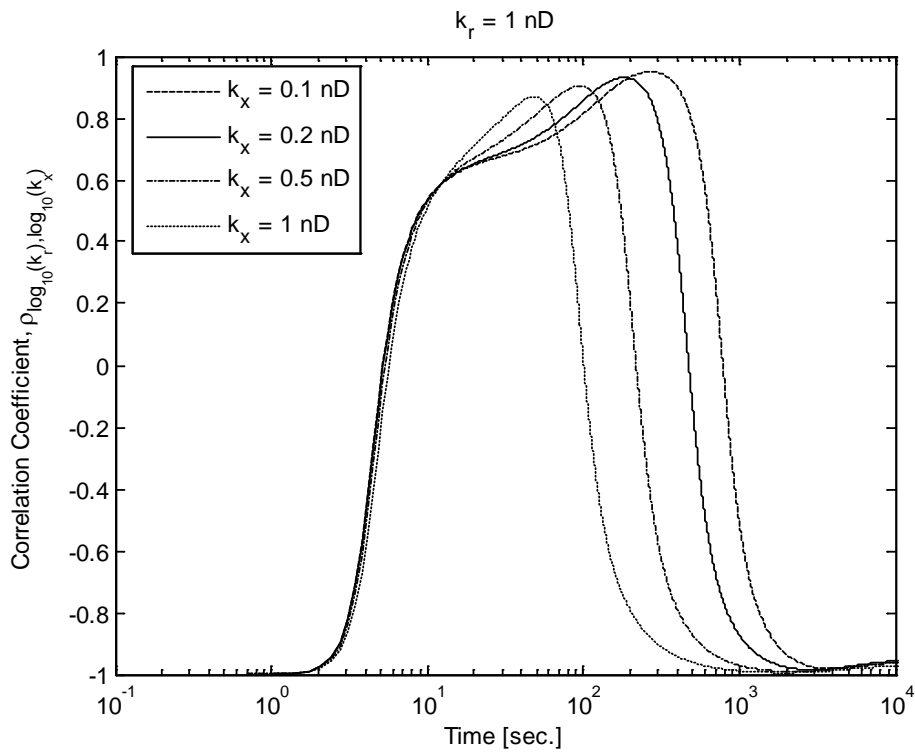


Figure 2.2.2. Correlation coefficient between the two principal permeabilities in the pressure-pulse-decay model.

3. Simulation of CO₂ Migration and Trapping in Storage Reservoirs and Leakage through Seal Layers

3.1. Simulation of CO₂ Injection into Middle Donovan Sands at Citronelle, Alabama, using TOUGHREACT*

Konstantinos Theodorou
Interdisciplinary Engineering Program
UAB

TOUGHREACT (Xu et al., 2004a, 2004b, 2004c) is a numerical simulator and extension of Lawrence Berkeley National Laboratory's TOUGH2 code (Pruess, Oldenburg, and Moridis, 1999; Pruess, 2005; Pruess and Spycher, 2006) having the ability to simulate chemical processes that occur during and after CO₂ injection into saline formations. A set of simulations was performed using TOUGHREACT to investigate the long-term behavior and fate of CO₂ sequestered in Middle Donovan Sands at Citronelle. The simulations began with a 40-year CO₂ injection period, followed by a shut-in period lasting 10,000 years.

The simulations of CO₂ injection into Middle Donovan Sands were performed using a two-dimensional symmetric radial grid with a single CO₂ injection well at the center. The radius of the grid extended to a large distance of 100,000 m from the injection well, to assure that the simulated system could maintain constant pressure at the boundary, acting as an infinite reservoir. The radius of the well was 0.07 m, and the grid block length was increased progressively, away from the wellbore, according to a logarithmic rule calculated by the simulator internally. The progressive increase in grid block length provided sufficient detail of the injection process near the high pressure well-bore region, while maintaining constant pressure at the boundary of the CO₂ plume. The simulations were performed using a CO₂ injection rate of 36.3 t/day (40 short tons/day), with the permeability reduction option enabled, and the van Genuchten parameter, m , set equal to 0.5.

Injected CO₂ was in the supercritical state, well above the critical temperature of 31.1 °C (87.98 °F) and critical pressure of 7.39 MPa (1071.8 psi). Table 3.1.1 summarizes the primary input variables, and their values, utilized in all of the simulations of CO₂ injection into the Middle Donovan Sands. The simulations were performed under isothermal conditions and under the assumption that the formation was homogeneous and isotropic. Gravity and inertial effects were neglected. As indicated in Table 3.1.1, the Middle Donovan formation is at a temperature of 98.9 °C (210 °F) and pressure of 34 MPa (4931.3 psi), above the critical temperature and pressure of CO₂.

*K. Theodorou, "Carbon Dioxide Enhanced Oil Recovery from the Citronelle Oil Field and Carbon Sequestration in the Donovan Sand, Southwest Alabama," Doctoral Dissertation, Interdisciplinary Engineering, University of Alabama at Birmingham, 2013.

Table 3.1.1. Primary input variables for the TOUGH2 simulations of carbon dioxide storage in Middle Donovan Sands.

Property	Value	Source
Formation thickness	27.6 m	Esposito et al., 2008
Porosity	13%	Esposito et al., 2008
Permeability	13 mdarcy	Esposito et al., 2008
Formation pressure	34 MPa (4931.3 psi)	Calculated hydrostatic
Formation temperature	98.9 °C (210 °F)	Esposito et al., 2008
NaCl mass fraction in brine	10 wt%	J. C. Pashin, personal communication, Aug. 2009

To simulate chemical processes, TOUGHREACT requires, as input, the initial volume fractions of the formation's primary mineral components, and their chemical kinetic properties. Table 3.1.2, summarizes the primary mineral components of the sandstones in the Rodessa Formation at the Citronelle Oil Field, and their average volumetric abundances, determined by David C. Kopaska-Merkel (Geological Survey of Alabama, personal communication, 2010). The chemical kinetic rate law parameters and reactive surface areas, used in the simulations for the mineral components listed in Table 3.1.2, were obtained from the TOUGHREACT manual (Xu et al., 2004b).

Table 3.1.2. Average initial volume fractions of primary mineral components identified in the sandstones of the Rodessa Formation in the Citronelle Oil Field (D. C. Kopaska-Merkel, Geological Survey of Alabama, personal communication, 2010).

Primary Mineral	Chemical Formula	Volume Fraction
Quartz	SiO ₂	0.44
Clay	Al ₂ (Si ₂ O ₅)(OH) ₄ (K,H ₃ O)(Al,Mg,Fe) ₂ (Si,Al) ₄ O ₁₀ [(OH) ₂ ,(H ₂ O)]	0.22
Feldspar	(K, Na, Ca)AlSi ₃ O ₈	0.14
Calcite	CaCO ₃	0.09
Mica	H ₂ KAl ₃ (SiO ₄) ₃ K(Mg, Fe ²⁺) ₃ (Al, Fe ³⁺) Si ₃ O ₁₀ (OH, F) ₂	0.04

Minerals that form and precipitate during and after CO₂ injection are classified as secondary by TOUGHREACT, and their formation depends on the primary minerals considered. Primary minerals can also dissolve and precipitate due to changing conditions and the chemical reactions induced by the injection of CO₂ into the medium. Based on the list of primary minerals shown in Table 3.1.2, the possible secondary minerals formed during and after CO₂ injection into the Middle Donovan are listed in Table 3.1.3. The minerals are the products of chemical reactions that take place as result of the CO₂ injection.

Table 3.1.3. Possible secondary minerals that could form during TOUGHREACT simulations of CO₂ injection into the Middle Donovan, based on the primary minerals of the Rodessa Formation in the Citronelle Field (Table 3.1.2).

Secondary Mineral	Chemical Formula
Magnesite	MgCO ₃
Dolomite	CaMg(CO ₃) ₂
Siderite	FeCO ₃
Dawsonite	NaAlCO ₃ (OH) ₂
Ankerite	CaMg _{0.3} Fe _{0.7} (CO ₃) ₂
Albite	NaAlSi ₃ O ₈
Ca-smectite	Ca _{0.145} Mg _{0.26} Al _{1.77} Si _{3.97} O ₁₀ (OH)
Pyrite	FeS ₂

Output from the simulations was obtained at 100, 1000, and 10,000 years. The parameters and properties of interest are: CO₂ saturation, dissolved CO₂ in the aqueous phase, secondary minerals produced by chemical reactions due to the presence of CO₂, yield of CO₂ in solid phases due to mineralization, and porosity and permeability changes associated with the chemical reactions.

Figure 3.1.1 shows the CO₂ saturation at 100, 1000, and 10,000 years. At 100 years, a dried-out region, from which liquid water was completely removed by evaporation into flowing CO₂ during injection, is still present out to a distance of approximately 9 m from the injection well. Beyond 9 m, to a distance of 500 m, is a transition region where supercritical CO₂ and CO₂-saturated brine coexist. At 1000 years, the dried-out region has been reinvaded by the aqueous phase, and the CO₂ saturation, from the wellbore out to approximately 20 m, is 32.4%. At 10,000 years, CO₂ saturation, from the wellbore out to approximately 200 m, is 12.7%, and the leading edge of the supercritical CO₂ plume is 680 m from the injection well.

Figure 3.1.2 shows the mass fraction of CO₂ dissolved in the aqueous phase at 100, 1000, and 10,000 years. The maximum dissolved CO₂ mass fraction is 5 wt%, in the region from roughly 10 to 500 m, where supercritical CO₂ and brine have both been present from early times. At 100 years, the trailing edge of the dissolved CO₂ plume is at 9 m, but it retracts at 1000 and

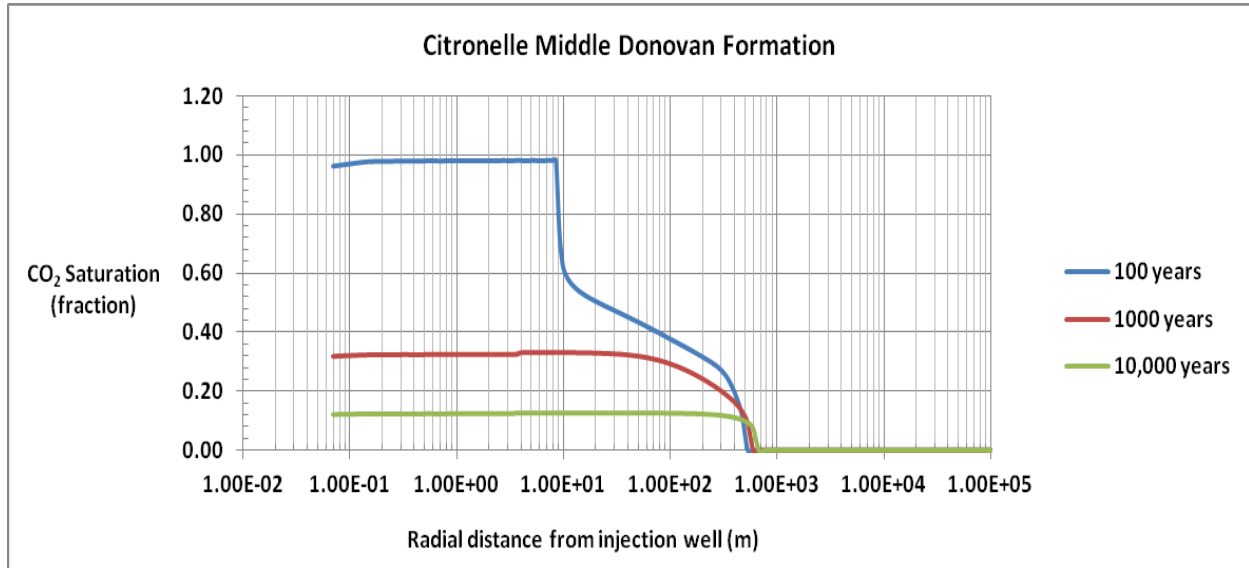


Figure 3.1.1. CO₂ saturation at 100, 1000, and 10,000 years. Citronelle Middle Donovan formation, TOUGHREACT simulations with permeability reduction enabled.

10,000 years, due to reinvasion of brine into the dried-out region. The lower dissolved CO₂ mass fraction at distances less than 3 to 4 m from the wellbore, at 1000 and 10,000 years, is due to lower CO₂ solubility in the presence of the higher NaCl concentration in that region resulting from the addition to the reinvading brine of NaCl left behind when the region close to the wellbore dried out. At 100 years there is no dissolved CO₂ near the wellbore because there is no water there. At 10,000 years the leading edge of the dissolved CO₂ plume is 767 m from the injection well, which is 87 m farther than the leading edge of the CO₂ saturation curve at the same time, as shown in Figure 3.1.1. The greater extent of the dissolved CO₂ plume, compared to the extent of the supercritical CO₂ plume, at 1000 and 10,000 years, is due to outward diffusion of CO₂ in the aqueous phase.

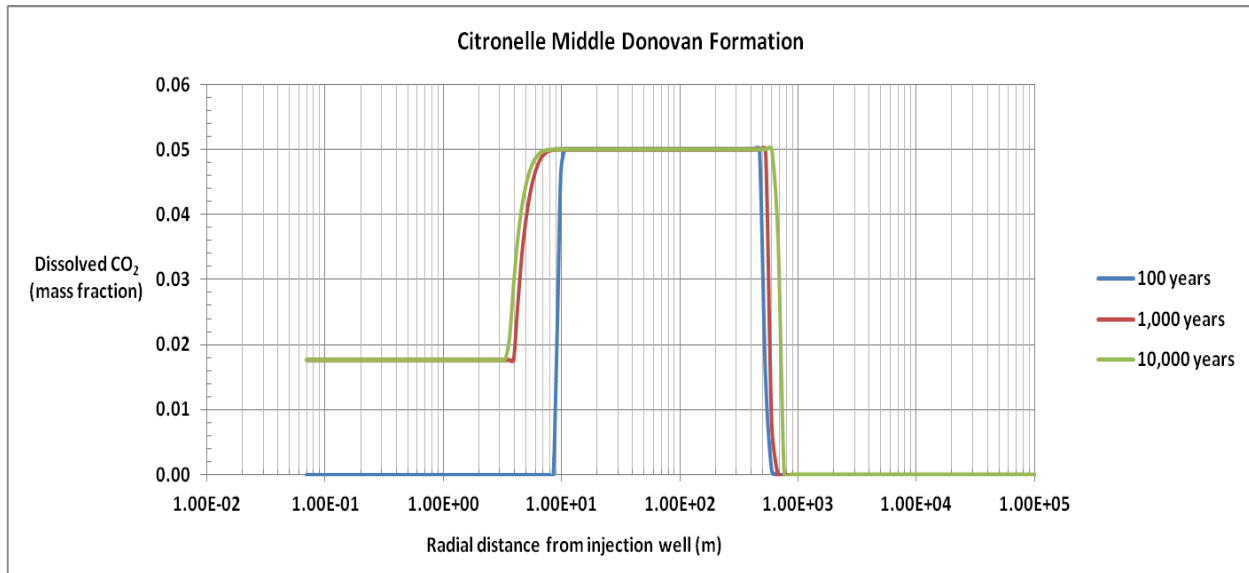


Figure 3.1.2. Dissolved CO₂ in the aqueous phase at 100, 1000, and 10,000 years. Citronelle Middle Donovan formation, TOUGHREACT simulations with permeability reduction enabled.

As CO₂ dissolves in the aqueous phase, it forms H⁺ and HCO₃⁻. These ions may react with minerals and, depending on the conditions and mineralogy of the formation, may induce precipitation of carbonate minerals such as ankerite, dawsonite, calcite, dolomite, and siderite, converting CO₂ into minerals.

The first five minerals listed in Table 3.1.3 are carbonate minerals in which CO₂ may be mineralized during and after CO₂ injection. However, not all of the possible secondary minerals listed in the table were found in the system. Two of the carbonate minerals, magnesite and dolomite, were not formed and did not contribute to CO₂ mineralization.

Minerals that did form during the simulation were siderite, dawsonite, and ankerite, and each of them contributed to the mineralization of CO₂. The abundances of siderite, dawsonite, and ankerite are shown in Figures 3.1.3, 3.1.4, and 3.1.5, respectively. The changes in dawsonite volume fraction (Figure 3.1.4) are larger than those of either siderite (Figure 3.1.3) or ankerite (Figure 3.1.5). Ankerite precipitation first increases at 1000 years, then decreases to minimal levels at 10,000 years, as a result of competition with siderite for iron.

Another mineral contributing to mineralization of CO₂ is the primary carbonate mineral calcite (CaCO₃), shown in Figure 3.1.6, which, after minor dissolution near the injection well and significant precipitation in the two-phase region at 100 years, increased in abundance throughout the region under consideration at 1000 and 10,000 years. Calcite is the mineral primarily responsible for mineralization of CO₂ in the "background" region, beyond the dissolved CO₂ front at 767 m from the injection well (Figure 3.1.2, 10,000 years), as was observed by Xu and coworkers (2004c). The source of calcium for the formation of calcite is dissolution of the feldspar mineral oligoclase (CaNa₄Al₆Si₁₄O₄₀), shown in Figure 3.1.7, whose correlation with formation of calcite can be seen by comparison with Figure 3.1.6.

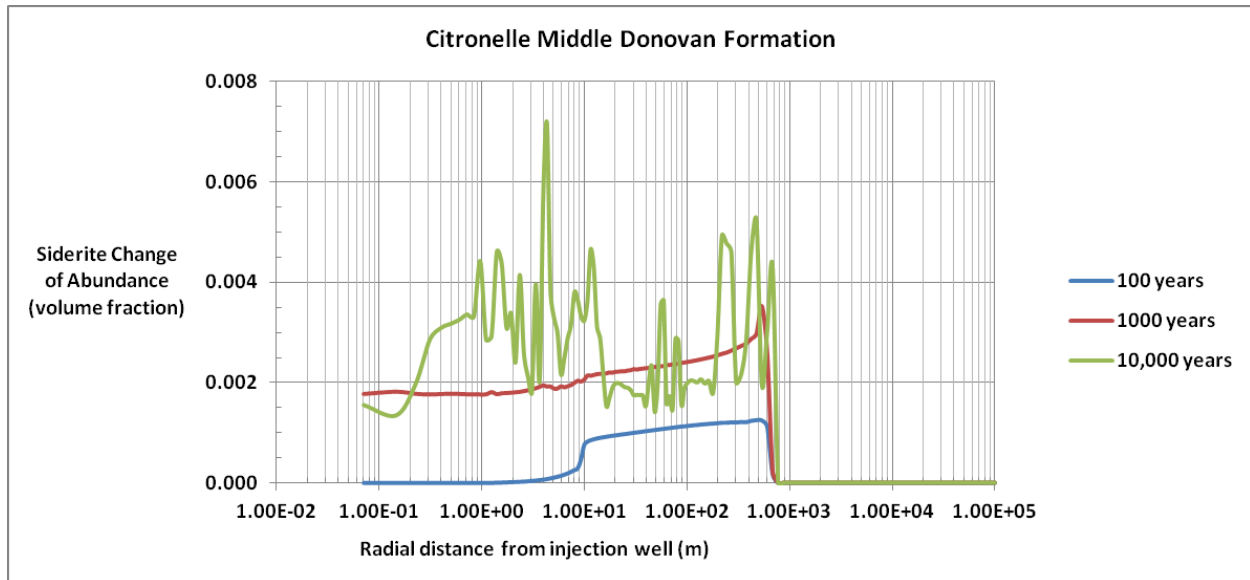


Figure 3.1.3. Siderite volume fractions at 100, 1000, and 10,000 years. Citronelle Middle Donovan formation, TOUGHREACT simulations with permeability reduction enabled.

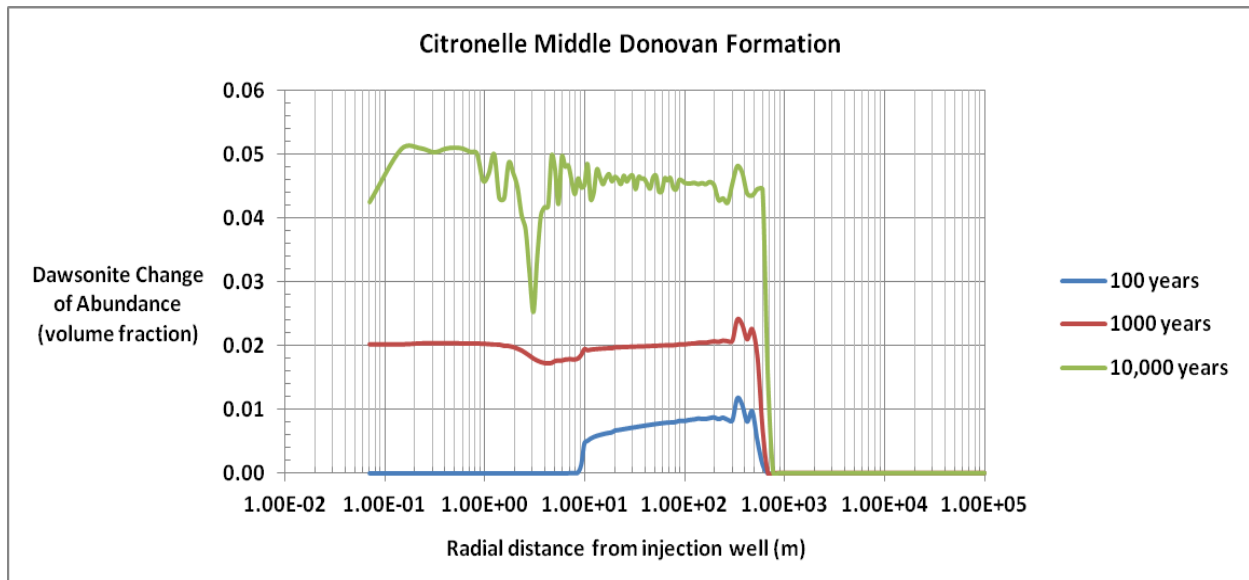


Figure 3.1.4. Dawsonite volume fractions at 100, 1000, and 10,000 years. Citronelle Middle Donovan formation, TOUGHREACT simulations with permeability reduction enabled.

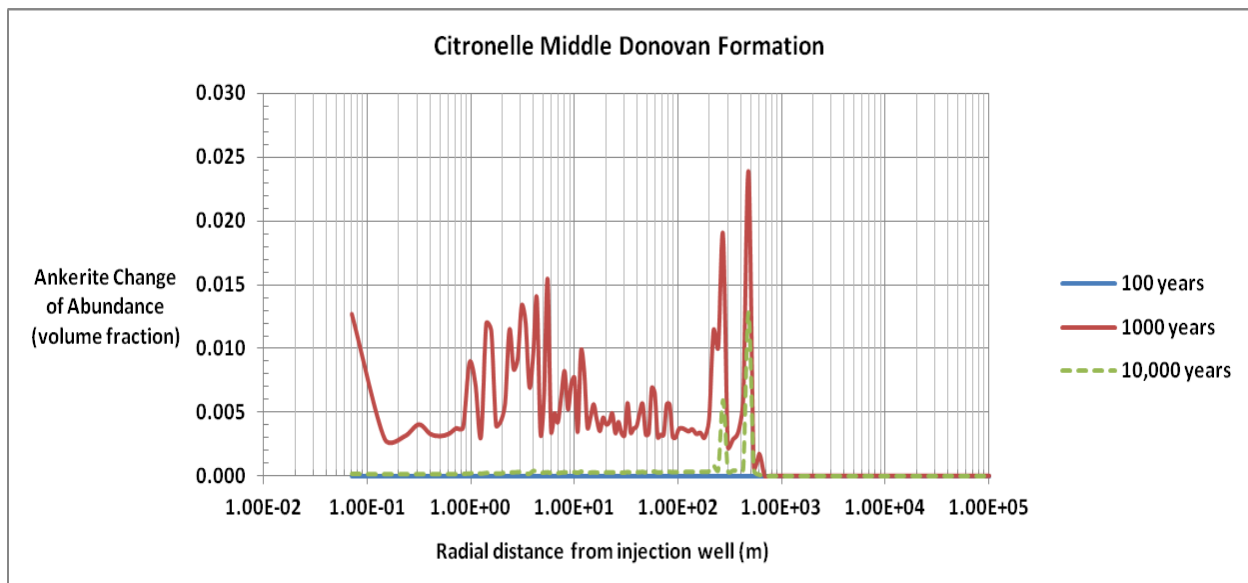


Figure 3.1.5. Ankerite volume fractions at 100, 1000, and 10,000 years. Citronelle Middle Donovan formation, TOUGHREACT simulations with permeability reduction enabled.

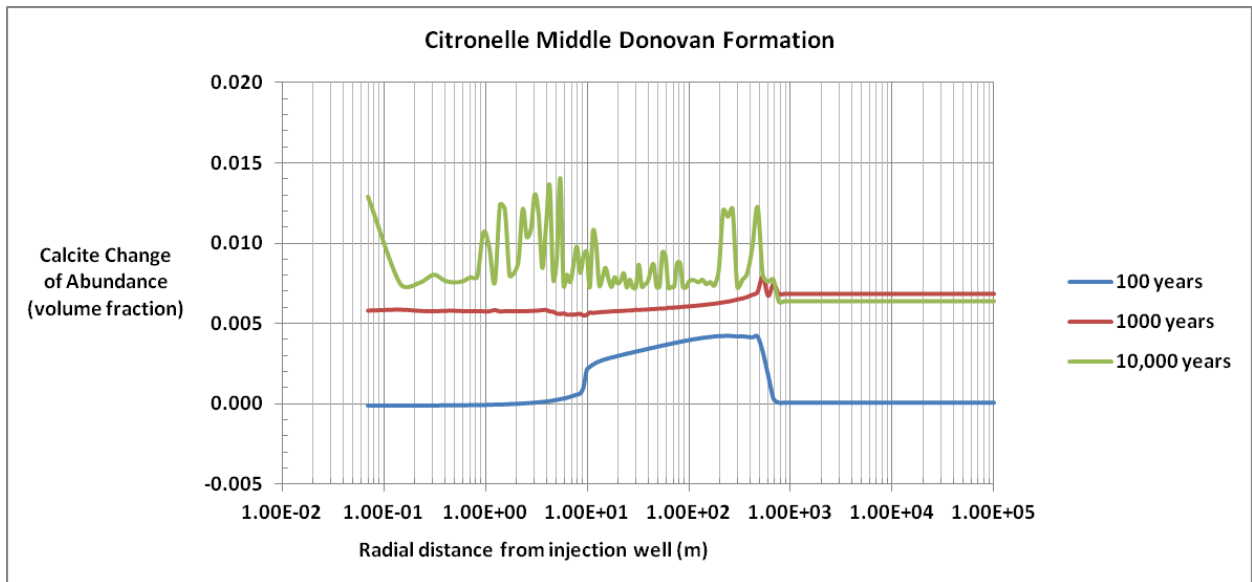


Figure 3.1.6. Calcite volume fractions at 100, 1000, and 10,000 years. Citronelle Middle Donovan formation, TOUGHREACT simulations with permeability reduction enabled. Positive values denote precipitation and negative values denote dissolution.

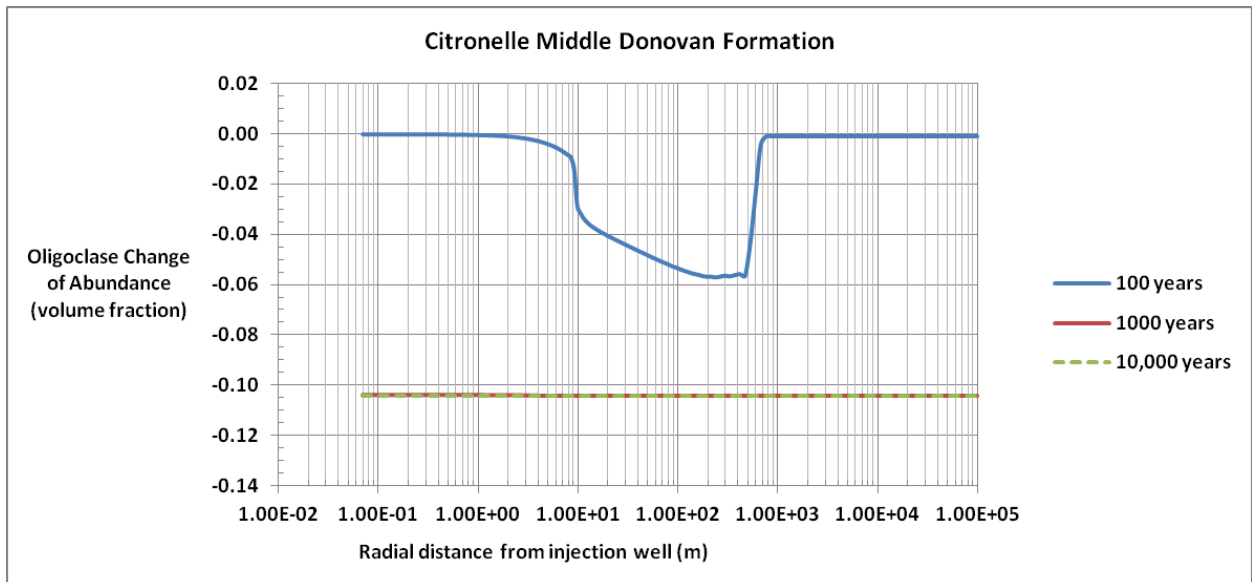


Figure 3.1.7. Oligoclase volume fractions at 100, 1000, and 10,000 years. Citronelle Middle Donovan formation, TOUGHREACT simulations with permeability reduction enabled. Positive values denote precipitation and negative values denote dissolution.

Two other minerals undergoing significant changes are quartz (SiO_2), shown in Figure 3.1.8, and clay in the form of kaolinite ($\text{Al}_2\text{Si}_2\text{O}_5(\text{OH})_4$), shown in Figure 3.1.9. Quartz is formed by dissolution of soluble components of silicate minerals. Quartz, clays, and feldspars comprise 80 vol% of the minerals in the sandstones of the Middle Donovan, as shown in Table 3.1.2. Formation and dissolution of these minerals affects porosity, permeability, and fluid flow.

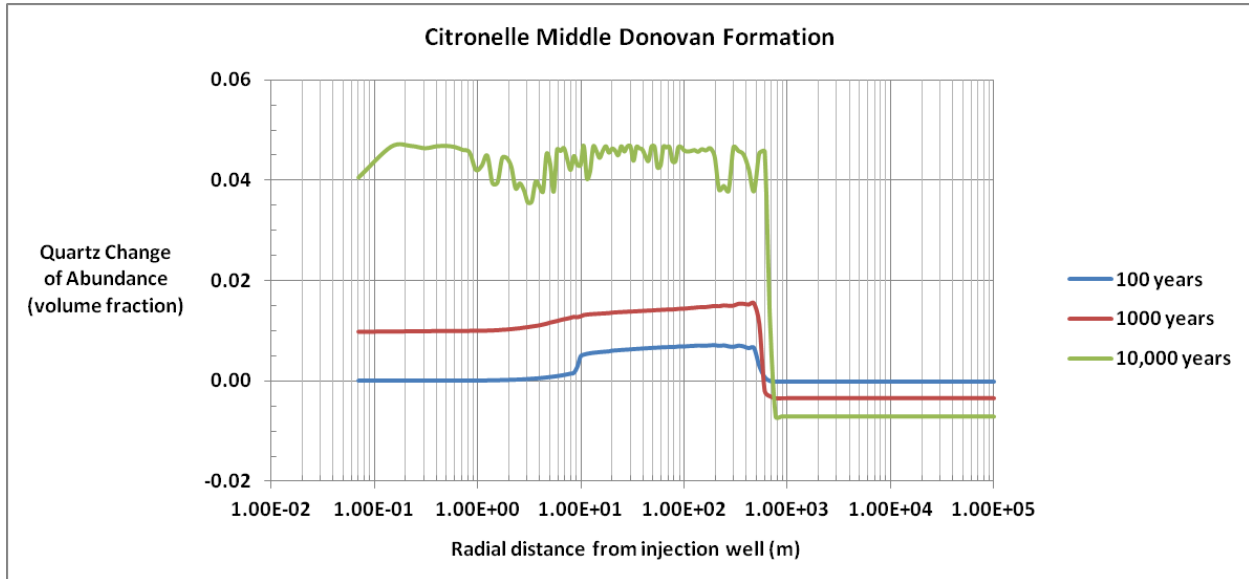


Figure 3.1.8. Quartz volume fractions at 100, 1000, and 10,000 years. Citronelle Middle Donovan formation, TOUGHREACT simulations with permeability reduction enabled. Positive values denote precipitation and negative values denote dissolution.

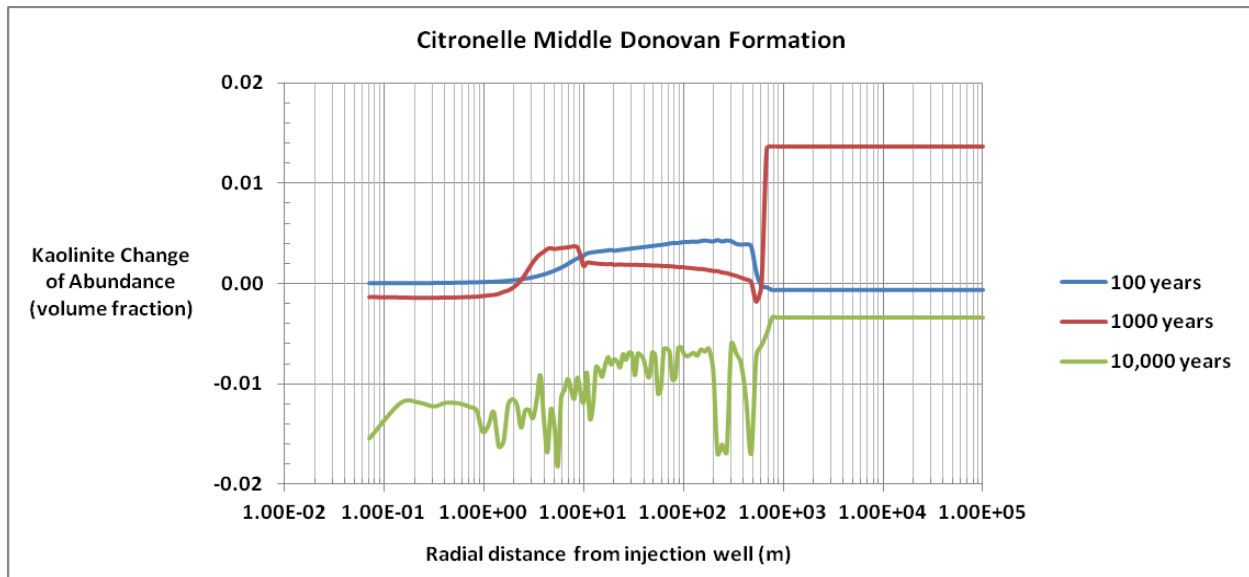


Figure 3.1.9. Kaolinite volume fractions at 100, 1000, and 10,000 years. Citronelle Middle Donovan formation, TOUGHREACT simulations with permeability reduction enabled. Positive values denote precipitation and negative values denote dissolution.

Porosity, shown in Figure 3.1.10, is unaffected near the injection well at 100 years, but decreases from its initial value of 13% to almost 12% near the leading edge of the CO₂ plume. At 1000 years, porosity decreases to 10.5% in the injection well grid block, due to formation of solid salt and precipitation of carbonate minerals. Porosity increases to 11.5% in the immediate vicinity of the well, but undergoes another significant decrease to 9.5% near the leading edge of the plume. At 10,000 years, porosity has decreased to an average of 10.5% within the CO₂ plume and to 12.8% in the region outside the plume, where changes associated with CO₂ injection have occurred, but where neither free supercritical CO₂ nor dissolved CO₂ are "visible."

Permeability, shown in Figure 3.1.11, follows trends similar to those of porosity. It is unaffected near the injection well at 100 years, remaining at its initial value of 13 mDarcy, but decreases to a low of 10.5 mDarcy near the leading edge of the CO₂ plume. In the injection well grid block it decreases to 7.1 and 6.7 mDarcy at 1000 and 10,000 years, respectively. At 10,000 years, permeability averages 7 mDarcy within the plume and 12.6 mDarcy in the brine-saturated region beyond the dissolved CO₂ front at ~800 m from the CO₂ injector.

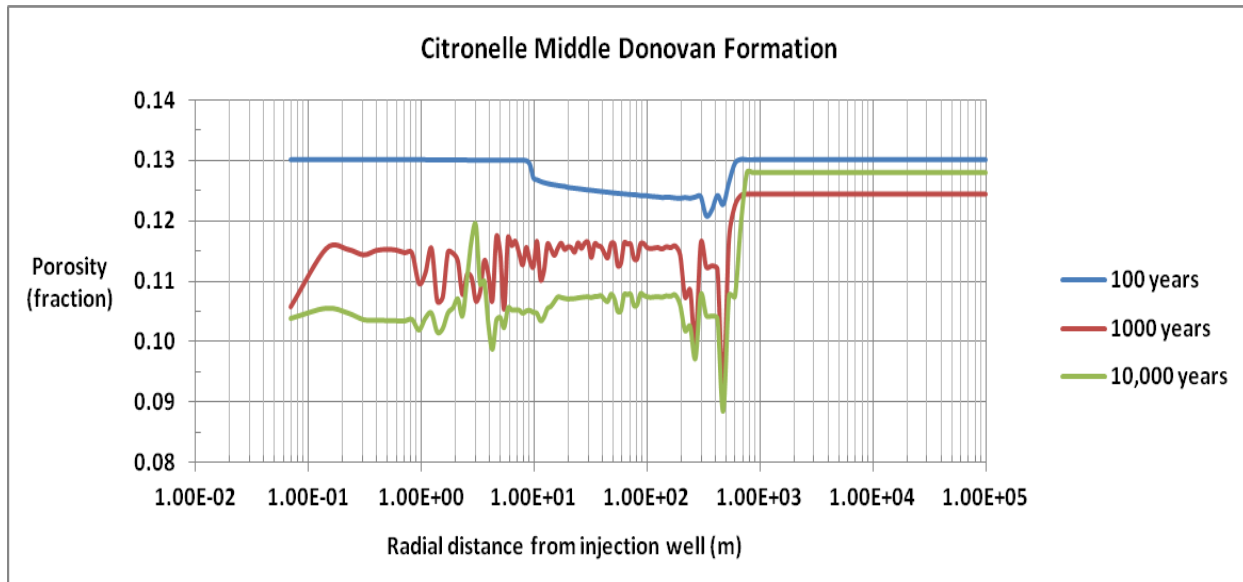


Figure 3.1.10. Porosity at 100, 1000, and 10,000 years. Citronelle Middle Donovan formation, TOUGHREACT simulations with permeability reduction enabled.

Dawsonite, calcite, siderite, and ankerite are the minerals responsible for conversion of CO₂ into solids, during and after CO₂ injection. The cumulative sequestration of CO₂ by carbonate formation is shown in Figure 3.1.12. Mineral trapping of CO₂ peaks at 73 kg/m³ of medium near the leading edge of the CO₂ plume at 10,000 years. The average value over the entire plume at 10,000 years is 50 kg/m³ of medium. Approximately 8 kg CO₂/m³ are mineralized as calcite in the brine-saturated region beyond the leading edge of the plume at 10,000 years, similar to the behavior in the background region of the system analyzed by Xu et al. (2004c).

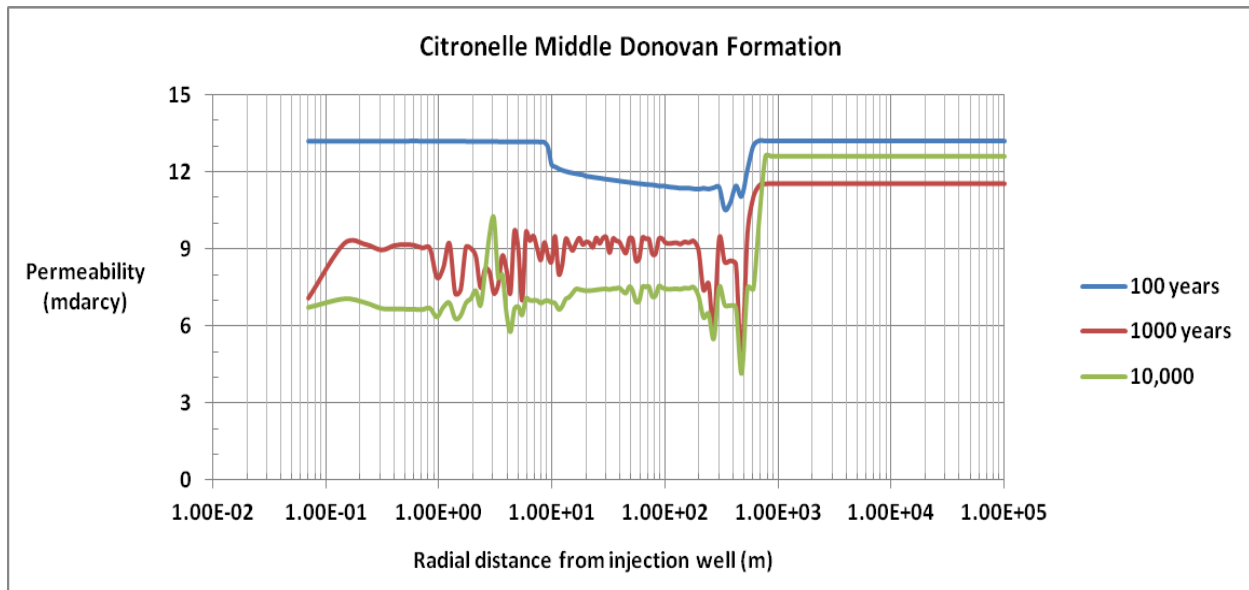


Figure 3.1.11. Permeability at 100, 1000, and 10,000 years. Citronelle Middle Donovan formation, TOUGHREACT simulations with permeability reduction enabled.

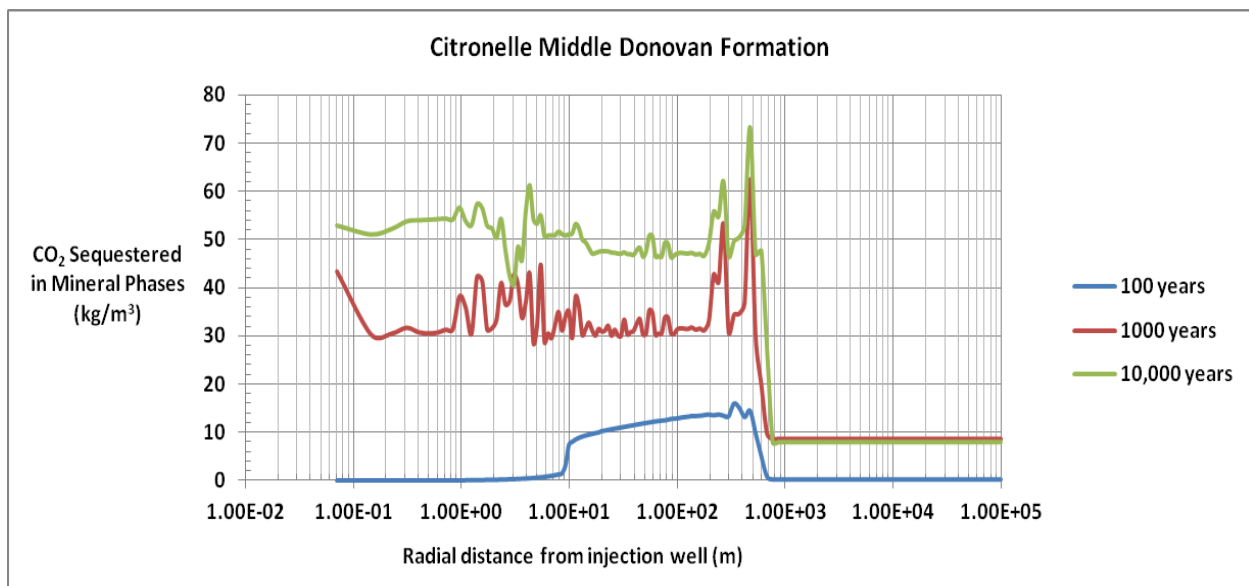


Figure 3.1.12. Cumulative CO₂ mineralization at 100, 1000, and 10,000 years. Citronelle Middle Donovan formation, TOUGHREACT simulations with permeability reduction enabled. Carbonate minerals were, in order of abundance (volume fraction) within the CO₂ plume at 10,000 years: dawsonite, calcite, siderite, and ankerite.

3.2. Effectiveness of Confining Layers: The Critical CO₂ Column Height

Konstantinos Theodorou

Department of Mechanical Engineering and Interdisciplinary Engineering Ph.D. Program
UAB

Peter M. Walsh

Department of Mechanical Engineering
UAB

Saline formations in Citronelle Dome, Southwest Alabama, are promising candidates for sequestration of CO₂ from coal-fired generation at Alabama Power Company's Plant Barry, 10 miles to the southeast. Esposito, Pashin, and Walsh (2008) estimated the CO₂ storage capacity of three groups of sands in Citronelle Dome: (1) Eutaw and Upper Tuscaloosa Sands at depths of approximately 5700 to 6400 ft, (2) Pilot and Massive Sands of the Lower Tuscaloosa Group at depths of approximately 6800 to 7200 ft, and (3) Upper, Middle, and Lower Donovan Sands of the Rodessa Formation at depths of approximately 10,600 to 11,600 ft. The geology of the formations is described in detail by Esposito et al. (2008). Their general structure is brine or oil-bearing sandstones separated by shale. Carbon dioxide storage capacities were estimated for the sandstones in each group: Eutaw and Upper Tuscaloosa Sands, 150 to 600 million short tons of CO₂; Pilot and Massive Sands, 240 to 950 short tons of CO₂; and Donovan Sands, 139 to 560 short tons of CO₂, for a total, in these sands alone, of 529 to 2110 short tons, sufficient to store the typical annual output of CO₂ from coal-fired generation at Plant Barry (10 million tons/year) for at least 50 years. A preliminary analysis was done to examine the ability of the shale layers to inhibit upward migration of CO₂ stored in the sandstones.

The effectiveness of a confining layer is a function of the difference in pressure required to drive a column of carbon dioxide from the pores of the storage reservoir, through pore throats in the seal. Under hydrostatic conditions, the forces acting are capillary pressures in the reservoir rock and caprock, and the buoyant force on the column of carbon dioxide, due to the difference between its density and that of surrounding brine. The problem was analyzed by Berg (1975), who derived the following equation for the critical height of a column of fluid capable of upward migration from a reservoir into barrier facies under hydrostatic conditions:

$$\text{Critical Height} = \frac{2\gamma \left[\frac{1}{r_{t, \text{cap}}} - \frac{1}{r_{p, \text{res}}} \right]}{g (\rho_{\text{brine}} - \rho_{\text{CO}_2})} \quad (3.2.1)$$

In the case that the reservoir fluid is CO₂, and the surrounding fluid is brine, γ is the surface tension of brine against CO₂, $r_{t, \text{cap}}$ is the radius of pore throats in the caprock, $r_{p, \text{res}}$ is the radius of pores in reservoir rock, g is the acceleration due to gravity, and ρ_{brine} and ρ_{CO_2} are the formation water and carbon dioxide densities, respectively, under reservoir conditions.

A substantial body of work exists on the interfacial properties of CO₂-water-mineral systems, motivated by the development of technology for geologic storage of carbon dioxide. See, for example, Chiquet et al. (2007), Kvamme et al. (2007), Chalbaud et al. (2009), Espinoza and Santamarina (2010), and Bikkina (2011). In particular, the work of Chalbaud et al. (2009)

gives the surface tension of CO₂-brine, under conditions typical of the reservoirs under consideration, as 0.026 N/m.

Pore throat radii in the seal and pore radii in the reservoir rock are given by the following relationships for rhombohedral packing of uniform-size spherical grains (Graton and Fraser, 1935):

$$r_{t, cap} = 0.5(0.154 D_{cap}) \quad (3.2.2)$$

$$r_{p, res} = 0.5(0.414 D_{res})$$

where D_{cap} and D_{res} are the grain diameters in cap and reservoir rock, respectively. In the absence of grain or pore size measurements, the effective grain size can be estimated using the following correlation (Berg, 1975):

$$D_e = 3.476 (k \varphi^{-5.1})^{1/2} \quad (3.2.3)$$

in which k is the permeability (m²) and φ is the porosity (dimensionless).

The following values of the parameters in Equations (3.2.1), (3.2.2), and (3.2.3) were estimated for the sandstone and shale units in Citronelle Dome:

- $k = 1.283 \times 10^{-14} \text{ m}^2 = 13 \text{ mdarcy}$, estimated average permeability of the sands.
- $\varphi = 0.20$, porosity of Eutaw, Upper Tuscaloosa, Pilot, and Massive Sands.
- 0.13, porosity of Upper, Middle, and Lower Donovan Sands.
- $D_{res} = D_e = 24 \text{ }\mu\text{m}$, grain size in Eutaw, Upper Tuscaloosa, Pilot, and Massive Sands,
- = 72 μm , grain size in Upper, Middle, and Lower Donovan Sands,
- Equation (3.2.3).
- $\rho_{brine} = 1000 \text{ kg/m}^3$, estimate of the density of brine at 5000 psig, 245 °F.
- $\rho_{CO_2} = 647 \text{ kg/m}^3$, Eutaw and Upper Tuscaloosa Sands,
- = 702 kg/m^3 , Pilot and Massive Sands,
- = 715 kg/m^3 , Upper, Middle, and Lower Donovan Sands (Lemmon et al., 2007).
- $\gamma = 0.026 \text{ N/m}$, surface tension of brine against CO₂ (Chalbaud et al., 2009).

Evaluation of the grain diameters in the caprocks remains a subject for future work. We take the effective grain size in the shale units as:

$$D_{cap} = 2 \text{ }\mu\text{m} \text{ (fine siltstone or shale)}$$

Site-specific porosities and permeabilities, grain sizes, or pore throat diameters in the shales can be determined by study of samples from the formations themselves.

Substitution of these values into Equations (3.2.2) and (3.2.1) gives estimates of critical CO₂ column heights of 95 m (Eutaw and Upper Tuscaloosa Sands), 112 m (Pilot and Massive Sands), and 120 m (Upper, Middle, and Lower Donovan Sands). Sand units in the Rodessa formation (Upper, Middle, and Lower Donovan Sands) are typically between 2.4 and 12.2 m (8 to 40 ft) thick separated by shale (Esposito et al., 2008). On the basis of the present estimates of critical CO₂ column height in the Donovan Sands, leakage of CO₂ through the shale layers is not expected, consistent with the observation by Esposito et al.: "Shale units in the Rodessa Formation apparently form effective reservoir seals locally," The Massive Sand, at 91 m (300 ft) thick (Esposito et al., 2008, Figure 5), appears to be the thickest, nearly continuous

sandstone unit among the formations under consideration, but the thickness, even of this sand, is below its estimated critical CO₂ column height. Further improvement of the model, by more accurate assessment of pore radii, especially in the shales, is recommended.

It is not known how vertical connectivity of sands might allow for increased effective CO₂ column heights. That question can only be answered by detailed reservoir simulations. However, should the sealing capacity of the shale units prove to be imperfect, each of the reservoirs under consideration has a very effective regional seal: the Selma Chalk for the Eutaw and Upper Tuscaloosa Sands, the Marine Tuscaloosa Shale for the Pilot and Massive Sands, and the Ferry Lake Anhydrite for the Upper, Middle, and Lower Donovan Sands.

3.3. Model for Leakage through a Seal Layer

Peter M. Walsh
 Department of Mechanical Engineering
 UAB

A model for CO₂ seepage by capillary flow thorough a seal layer was based upon the model of Hildenbrand, Schlömer, Krooss, and Littke (2004). These authors treat injected CO₂ as forming a simple column in the subsurface having constant cross section. The rate of CO₂ storage, expressed as its mass per unit time per unit plan area of the reservoir, is the difference between the injection and leakage rates:

$$\text{storage rate} = \text{injection rate} - \text{leakage rate} \quad \text{kg}/(\text{m}^2 \cdot \text{s}) \quad (3.3.1)$$

The excess pressure, p , at the reservoir/seal layer interface, arising from the injection and accumulation of CO₂ beneath the seal, is:

$$p = (\rho_{brine} - \rho_{CO_2}) \cdot g \cdot \text{height of CO}_2 \text{ column} \quad (3.3.2)$$

Leakage begins when the excess pressure exceeds the minimum capillary displacement pressure, p_d , of the seal, at the critical CO₂ column height, which is related to fundamental physical properties of the system as described in Section 3.2. When the sizes of pores in the reservoir rock are much larger than the sizes of pore throats in the seal layer, the minimum capillary displacement pressure depends, according to Equations (3.2.1) and (3.3.2), only on the radii of pore throats in the seal and the surface tension of brine against CO₂. Equation (3.2.1) is based on the assumption that the contact angle between the wetting phase, brine in this case, and the minerals of the pore walls is small, and that the cosine of the contact angle is approximately equal to one.

The dependence of effective permeability on the excess pressure, above the minimum capillary displacement pressure, is described by a quadratic equation derived from measurements of pressure-pulse decay on a brine-saturated core, such as those discussed in Section 1.6 and shown in Figure 1.6.1:

$$\frac{k_{eff}}{k_{eff,max}} = 2 \left(\frac{p-p_d}{p_{max}-p_d} \right) - \left(\frac{p-p_d}{p_{max}-p_d} \right)^2 \quad p_d \leq p \leq p_{max} \quad (3.3.3)$$

The effective permeability of a seal layer is zero for excess pressures less than the minimum capillary displacement pressure. Above the minimum capillary displacement pressure, the effective permeability increases with increasing CO₂ column height up to the excess pressure, p_{max} , at which the irreducible brine saturation and maximum supercritical or gas-phase CO₂ saturation are reached. The effective permeability remains at its maximum value, $k_{eff,max}$, with further increase in CO₂ column height and increase in excess pressure above p_{max} :

$$k_{eff} = k_{eff,max} \quad p \geq p_{max} \quad (3.3.4)$$

The minimum capillary displacement pressure and maximum effective permeability were obtained from the absolute permeability using correlations given by Hildenbrand et al. (2004) for CO₂. To complete the definition of the system, we also require a relationship between p_{max} , the capillary pressure at which the maximum effective permeability is reached, and the minimum capillary displacement pressure, p_d . Based on only two measurements of the maximum effective

permeability in our laboratory and one set of measurements by Hildenbrand et al. (2004, Figure 3), we take $p_{max}/p_d \cong 6$, for the purposes of the present discussion. This relationship has no general validity, but would be determined directly, from measurements of p_d and p_{max} for a seal layer of interest.

The following conditions were adopted for the calculations presented here:

Porosity of the storage reservoir: 0.20

Depth at the bottom of the seal layer: 2875 m

Absolute permeability of the seal layer: 0.5, 1, and 2 μ darcy

Seal layer thickness: 1, 2, 5, 10, 20, and 50 m

CO₂ injection rate and time: 0.677 metric ton/(m²·year) for 10 years. The injection rate corresponds to 300 metric ton/day into wells on 40-acre centers.

Maximum CO₂ column height at 10 years, when injection is complete, in the absence of leakage: 54 m

Minimum capillary displacement pressure, maximum effective permeability, critical CO₂ column height, and time to breakthrough are given in Table 3.3.1, for each of the assumed values of absolute permeability.

Table 3.3.1. Minimum capillary displacement pressure, maximum effective permeability, critical CO₂ column height, and time to breakthrough for seal layers having absolute permeabilities of 0.5, 1, and 2 μ darcy, under the conditions specified in the text.

Property	----- Absolute Permeability -----		
	0.5 μ darcy 4.93 x 10 ⁻¹⁹ m ²	1.0 μ darcy 9.87 x 10 ⁻¹⁹ m ²	2.0 μ darcy 1.97 x 10 ⁻¹⁸ m ²
Minimum capillary displacement pressure ^a	243,089 Pa 35.3 psi	182,955 Pa 26.5 psi	137,696 Pa 20.0 psi
Maximum effective permeability ^{a,b}	0.053 μ darcy 5.27 x 10 ⁻²⁰ m ²	0.123 μ darcy 1.21 x 10 ⁻¹⁹ m ²	0.282 μ darcy 2.78 x 10 ⁻¹⁹ m ²
Critical CO ₂ column height	55.2 m	41.5 m	31.3 m
Time to breakthrough	no breakthrough	8 years	6 years

a. The minimum capillary displacement pressure and maximum effective permeability were obtained from the absolute permeability using correlations given by Hildenbrand et al. (2004) for CO₂.

b. The maximum effective permeability was assumed to be reached at a capillary pressure equal to six times the minimum capillary displacement pressure.

When the absolute permeability of the seal layer is 0.5 μ darcy, the critical CO₂ column height at breakthrough is estimated to be 55.2 m, which is greater than the height of the CO₂ column reached after injection of CO₂ at the assigned rate for 10 years. Although it is closely approached, CO₂ breakthrough is not expected through a seal having absolute permeability of 0.5 μ darcy under the assumed conditions. On the other hand, seals having absolute permeabilities of 1 and 2 μ darcy do permit leakage of CO₂, as shown in Figure 3.3.1.

The performance of seals having absolute permeability of 1 μ darcy is shown in Figure 3.3.1a. As shown in the figure and in Table 3.3.1, leakage begins at 8 years, toward the end of the injection period, when the excess pressure on the underside of the seal, due to the height of the CO₂ column, reaches the minimum capillary displacement pressure. For a seal layer having an absolute permeability of 1 μ darcy and thickness of 1 m, only 96.8% of injected CO₂ is expected to remain stratigraphically trapped after 100 years. As can be seen in the figure, capillary flow through the seal decreases with increasing thickness of the seal. A seal 5 m thick is expected to retain 99.2% of injected CO₂ at 100 years.

Increasing the absolute permeability of the seal to 2 μ darcy increases the rate of leakage markedly, as shown in Figure 3.3.1b. In this case, leakage begins 6 years into the 10-year injection period. A 5-m-thick seal is now able to retain only 95.9% of injected CO₂ at 100 years, corresponding to a loss five times greater than that through the seal having permeability only a factor of 2 smaller and the same thickness. Retention of 99% of injected CO₂ at 100 years is now achieved only by a seal layer having thickness greater than 50 m.

The properties of a seal layer may evolve, by reaction of its minerals with CO₂ and brine. A possible sequence of changes in brine-saturated pores accompanying CO₂ breakthrough and capillary flow through a seal is shown in Figure 3.3.2. Beginning on the left, with Figure 3.3.2a, a seal is able to remain fully saturated with brine, preventing capillary flow of gas-phase or supercritical CO₂, up to the capillary pressure at the smallest pore throat in the highest conductivity pore connecting the lower and upper faces of the seal. When the minimum capillary displacement pressure is exceeded, CO₂ enters and drains brine from the largest pores, leaving residual brine on the pore walls, saturated with CO₂ (Figure 3.3.2b). Interaction of dissolved CO₂ with solutes such as Ca²⁺(aq) in the brine and with minerals in the pore wall may lead to precipitation of carbonates, formation of carbonates from minerals in the wall, and dissolution of minerals soluble in the CO₂-saturated brine (Figure 3.3.2c). If the pressure on the underside of the seal remains above the minimum capillary displacement pressure, CO₂ continues to flow through, evaporating water from the brine and precipitating dissolved solids. The brine may eventually be completely dried out, leaving its dissolved solids on the pore walls, as shown in Figure 3.3.2d. If CO₂ injection were discontinued and the height of the CO₂ column began to decrease, due to leakage or spreading of the plume, pores that were drained by CO₂ would reimbibe brine, beginning with the smallest of the open pores. If the CO₂ column returned to its critical height, and the excess pressure on the underside of the seal returned to the minimum capillary displacement pressure, the largest of the drained pores would be filled again with brine, returning the seal to a condition similar to its original, brine-saturated state, as shown in Figure 3.3.2e. Some CO₂ would be likely to remain in the seal layer by residual and solubility trapping.

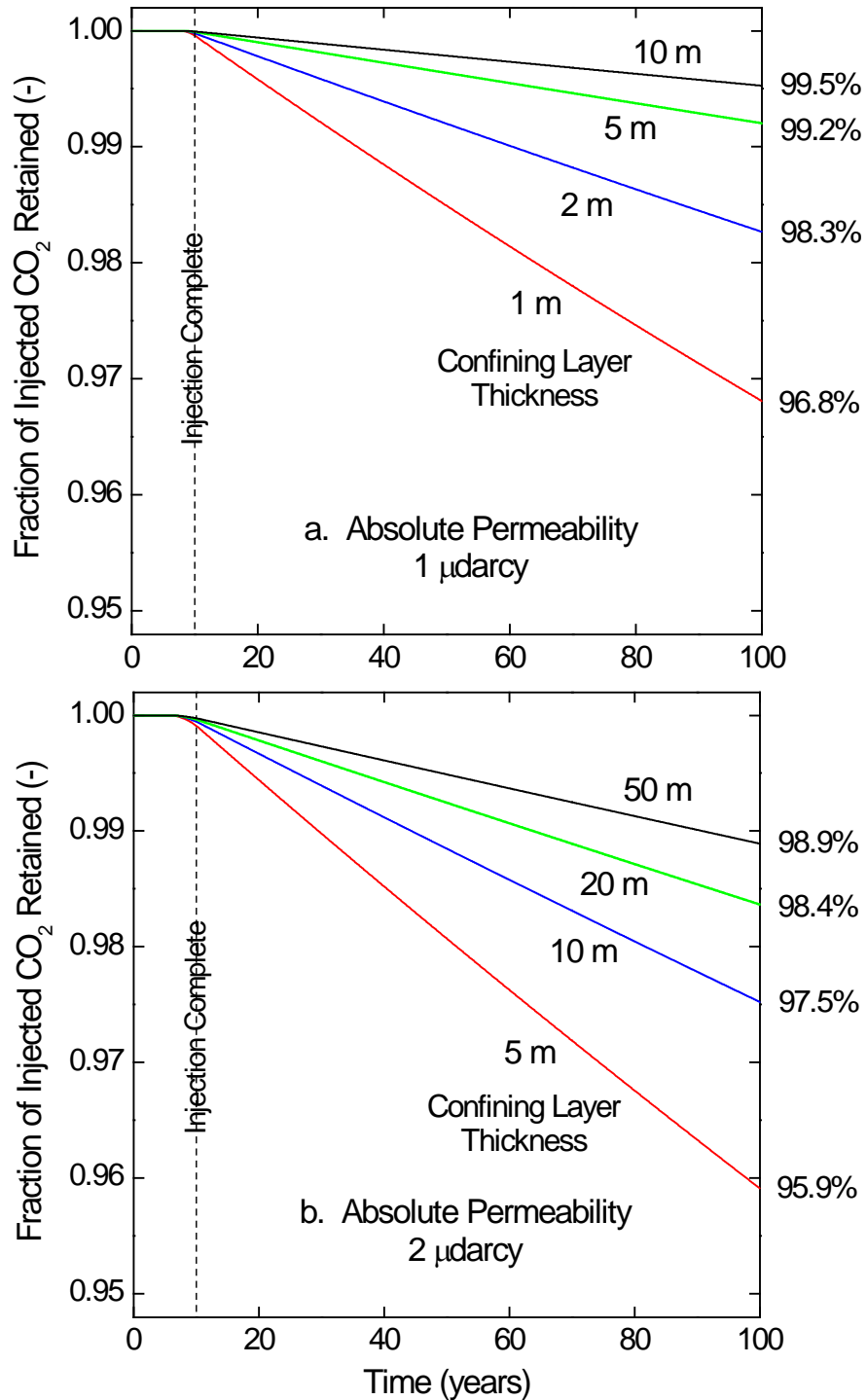
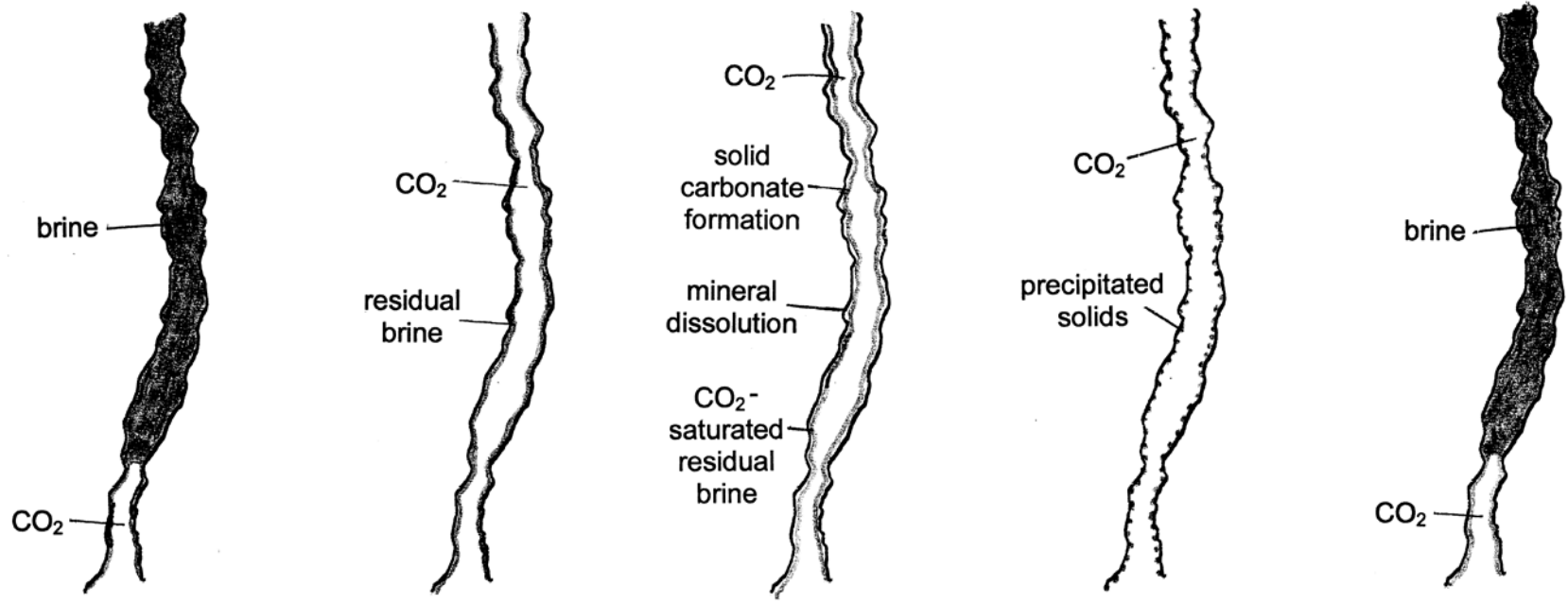


Figure 3.3.1. Model calculations of CO₂ leakage by capillary flow through seal layers as functions of permeability, thickness, and time. The fraction of injected CO₂ retained under each seal by stratigraphic trapping at 100 years is shown on the right.

- a. Absolute permeability 1 μ darcy and thickness of 1, 2, 5, and 10 m.
- b. Absolute permeability 2 μ darcy and thickness of 5, 10, 20, and 50 m.



a. Minimum capillary displacement pressure, p_d . Capillary pressure at the smallest throat in the highest conductivity pore.

b. Breakthrough at capillary pressure $p \geq p_d$.

c. CO_2 saturates residual brine on pore walls and may react with minerals in the walls and precipitate solids from the brine.

d. Brine dries out and leaves its dissolved solids on pore walls.

e. Decrease in CO_2 column height due to leakage or spreading of plume allows re-imbibition of brine.

Figure 3.3.2. Evolution of a brine-saturated pore in a seal layer in the presence of CO_2 , with the height of CO_2 column under the seal first increasing with increasing CO_2 storage, then decreasing as the CO_2 plume leaks or spreads.

4. Student Training

4.1. Student Training through Research

Four graduate students and one undergraduate student conducted research in connection with this project, described below. Two students were awarded Ph.D. degrees for their work.

Richard A. Esposito, Principal Research Geologist with Southern Company and Senior/Key Co-Investigator on the present project, completed the requirements for the Ph.D. in Interdisciplinary Engineering, defended his dissertation, and graduated in December 2010. Dr. Esposito's dissertation is entitled: "Business Models for Commercial-Scale Carbon Dioxide Sequestration; with Focus on Storage Capacity and Enhanced Oil Recovery in Citronelle Dome" (Esposito, 2010). Dr. Esposito has published several papers presenting the results of his research. The first, with coauthors L. S. Monroe and J. S. Friedman, is entitled, "Deployment Models for Commercialized Carbon Capture and Storage," published in *Environmental Science & Technology* (Esposito et al., 2011a). The paper describes and compares the options for physical deployment of carbon capture and storage and the business models that electric utilities may choose to adopt for management and sequestration of carbon dioxide from combustion of fossil fuels. Another paper, with coauthors R. Rhudy, R. Trautz, G. Koperna, and G. Hill, entitled, "Integrating Carbon Capture with Transportation and Storage," was presented at the 10th International Conference on Greenhouse Gas Control Technologies in Amsterdam and published in *Energy Procedia* (Esposito et al., 2011b). This paper discusses the unique aspects of the integration of carbon dioxide capture at electric power plants with pipeline transport and injection into saline formations. It includes a detailed discussion of the demonstration of CO₂ capture from Alabama Power Company's Plant Barry, transport of the CO₂ by pipeline to the Citronelle Oil Field in Southwest Alabama, and sequestration of the CO₂ in a saline formation in Citronelle Dome. Dr. Esposito also presented a paper, with coauthors C. Harvick, R. Shaw, D. Mooneyhan, R. Trautz, and G. Hill, at the 11th International Conference on Greenhouse Gas Technologies in Kyoto, November 18-22, 2012, entitled, "Integration of Pipeline Operations Sourced with CO₂ Captured at a Coal-Fired Power Plant and Injected for Geologic Storage: SECARB Phase III CCS Demonstration" (Esposito et al., 2013). The paper presents a detailed account of the planning, permitting, and start-up of the SECARB Phase III Plant Barry-Citronelle CCS Demonstration.

Konstantinos Theodorou completed the requirements for the Ph.D. in Interdisciplinary Engineering, defended his dissertation, and graduated in August 2013. The subject of Dr. Theodorou's research was a reservoir simulation study of CO₂-enhanced oil recovery from the Citronelle Oil Field and CO₂ storage in the Donovan Sands in Citronelle Dome (Theodorou, 2013), including detailed assessments of oil recovery, CO₂ storage capacity, and potential for leakage. Dr. Theodorou's calculations, using the TOUGHREACT simulator from LBNL, of CO₂ saturation, solution trapping, mineralization, and changes in porosity and permeability associated with chemical reactions between CO₂, brine, and minerals over long time scales (100,

1000, and 10,000 years) are discussed in the present report, in Section 3.1. His estimates of the critical heights of CO₂ columns that can be retained, without leakage, by seal layers above saline formations in Citronelle Dome, are also included in the present report, in Section 3.2.

Michael J. Hannon, Jr., is a candidate for the Ph.D., working on experimental measurement of caprock properties and the development of a new, less time-consuming measurement technique, capable of determining both axial and radial permeabilities of a cylindrical core plug in a single experiment, presented in Section 2 of this report. His analysis of transient pressure-pulse measurements using the equipment that he assembled for continuous measurement and acquisition of data for determination of porosity, permeability, and capillary displacement pressures is also included in the present report, in Section 1.3. Mr. Hannon presented and successfully defended his research proposal for Admission to Candidacy for the Ph.D. in May 2013. The subject of his proposal is the evaluation of alternatives to traditional methods for determining porosity and permeability of tight rocks. Mr. Hannon was awarded Second Place for his presentation entitled: "Simultaneous Determination of Porosity and Anisotropic Permeability of Cylindrical Core Shale Samples," at the Competition for Doctoral Students in February 2012, during Graduate Student Research Days, the annual symposium for presentation of research by UAB graduate students. He gave a poster presentation of his work, entitled "Sensitivity Analyses of a Fully Immersed Pressure-Pulse Decay Experiment on Cylindrical Samples of Layered Porous Media," at the Inverse Problems Symposium in Huntsville, AL, June 9-11, 2013 (Hannon, 2013). Mr. Hannon was named Outstanding Graduate Student in the UAB Interdisciplinary Engineering Ph.D. Program for 2013.

Kirk M. Ellison received a Master's Degree in 2011, for his research with Ronald W. Falta in the Department of Environmental Engineering and Earth Science at Clemson University. Mr. Ellison's thesis is entitled, "Risks Posed to Drinking Water Aquifers due to Leakage of Dissolved CO₂ in Improperly Abandoned Wellbores" (Ellison, 2011). Mr. Ellison is now a Research Scientist at Southern Company and working toward his Ph.D. in Interdisciplinary Engineering at UAB. He is preparing the proposal to his graduate program supervisory committee for research on permanent storage of solid waste from coal-fired electric power generation and modeling and simulation of CO₂ storage in geologic formations, with validation using results from the large-scale demonstration of carbon capture, transportation, and storage being conducted by SECARB, U.S. DOE, NETL, Southern States Energy Board, Advanced Resources International, Alabama Power Company, Denbury Resources, EPRI, Geological Survey of Alabama, Southern Company, and Southern Natural Gas at Alabama Power Plant Barry and the Citronelle Oil Field, north of Mobile, AL.

Aaron D. Lamplugh was an undergraduate student in the Global and Community Leadership Honors Program at UAB. He worked on the experimental measurement of permeability and tested the apparatus for measurement of the permeability of tight rocks by steady flow. Mr. Lamplugh's poster presentation on his independent study project, "Sealing Capacity of Confining Layers," at UAB EXPO, the University's Annual Exposition of Undergraduate Scholarship, in April 2011, was awarded Third Place and the award for "Most Interesting Graphics on Poster" in the Engineering Competition Area. Mr. Lamplugh graduated from UAB in May 2012. He is now with the U.S. Department of Transportation John A. Volpe National Transportation Systems Center in Cambridge, MA, working on improvement of transportation safety.

4.2 Student Training through Formal Course Work

Peter M. Walsh
Department of Mechanical Engineering
UAB

Richard A. Esposito
Senior/Key Co-Investigator
Principal Research Geologist
Southern Company

The advanced undergraduate/graduate course on coal combustion and gasification, climate change, and carbon sequestration, developed under the present project and first offered during the Fall Semester 2010, was offered for the second time during the Fall Semester 2012. The syllabus for the course is shown in Table 4.2.1. Seventeen undergraduates and eight graduate students completed the course in 2010 and sixteen undergraduates and eight graduate students completed the course in 2012. It has become a popular advanced thermal-fluid-sciences elective course in the Department of Mechanical Engineering.

Course work by the students includes eight homework assignments, two exams, and a final exam focused on pulverized coal combustion and integrated gasification-combined cycle systems for electric power generation, including carbon capture and storage. The course features a tour of Alabama Power Plant Miller and a guest lecture on carbon capture and sequestration by Dr. Richard Esposito, Principal Research Geologist with Southern Company and Senior/Key Co-Investigator on the present project. Student ratings of the course were good (4.87 and 4.82 out of 5.00). A student in the Fall 2010 class wrote, on her application to graduate school: "I was excited to learn that my interest in combustion products, their effects on the atmosphere, and methods of capturing them, could be turned into a career in science"

The recent shift by electric utilities from coal to natural gas suggests that future offerings of the course should place more emphasis on natural gas combined cycle power systems.

Table 4.2.1. The University of Alabama at Birmingham, August 21, 2012
ME 445/545 Combustion, Fall 2012, Course Outline

Date	Day	Meeting No.	Lecture Topic or Exam	Assignment Due
8/16	Thurs		No Class - Instructor out of town	
8/21	Tues	1	Applications of combustion, Primary energy flows, Fuel reserves and resources	
8/23	Thurs	2	Lifetimes of reserves, Population and economic growth	
8/28	Tues	3	Carbon content of fuels, Heating value, Carbon dioxide emissions, Greenhouse effect	
8/30	Thurs	4	Coal-fired electric power plant, Composition of coal, Stoichiometric air	Prob Set 1
9/4	Tues	5	Composition of combustion products, Adiabatic flame temperature	
9/6	Thurs	6	Boiler furnace, Coal preparation, Particle size distribution of pulverized coal	Prob Set 2
9/11	Tues	7	Coal burners, Flame structure, Free turbulent jets, Gas velocity distribution in free jets	
9/13	Thurs	8	Review	Prob Set 3
9/18	Tues	9	Swirling turbulent jets, Entrainment, Recirculation	
9/20	Thurs	10	Exam 1	
9/25	Tues	11	Residence time, temperature, and concentration distributions in jets	
9/27	Thurs	12	Heating of particles, ignition, devolatilization, and combustion of volatile matter	
10/2	Tues	13	Sizes of char residues, Kinetics of char combustion	
10/4	Thurs	14	Char burnout time, Size distribution of unburned char, Fraction of char unburned	Prob Set 4
10/9	Tues	15	Characteristic times and progress of combustion	
10/11	Thurs		Fall Break	
10/16	Tues	16	Radiative transfer, Flame temperature, NO _x formation	
10/18	Thurs	17	Inorganic matter in coal, Ash fusion temperatures, Furnace exit gas temperature	Prob Set 5
10/23	Tues	18	Energy balance on a boiler furnace, Resistance to heat transfer from a layer of ash or slag	
10/25	Thurs	19	Review	Prob Set 6
10/30	Tues	20	Staged combustion for NO _x reduction, Selective catalytic reduction of NO _x	
11/1	Thurs	21	Exam 2	
11/6	Tues	22	Separation of particles from combustion products, Scrubbing for removal of SO ₂	
11/8	Thurs	23	Greenhouse gases and climate change revisited	
11/13	Tues	24	Approaches to control of carbon dioxide emissions, Firing coal with oxygen	
11/15	Thurs	25	Natural gas-Combined cycle	Prob Set 7
11/20	Tues	26	Synthetic fuel gas from coal	
11/22	Thurs		Thanksgiving Holiday	
11/27	Tues	27	Integrated gasification and combined cycle	
11/29	Thurs	28	Separation and sequestration of carbon dioxide	
12/4	Tues	29	Review	Prob Set 8
12/11	Tues		Final Exam, 4:15 - 6:45 p.m.	

5. Technology Transfer

Technology transfer activities and events associated with the project are described below in chronological order, beginning with the most recent.

The Principal Investigator attended the 2013 Carbon Storage R&D Project Review Meeting in Pittsburgh on August 20-22 and presented the project during the ARRA WebEx Project Review Meeting on September 16, 2013.

Konstantinos Theodorou presented and successfully defended his doctoral dissertation in Interdisciplinary Engineering, entitled "Carbon Dioxide Enhanced Oil Recovery from the Citronelle Oil Field and Carbon Sequestration in the Donovan Sand, Southwest Alabama," on July 10, 2013. Dr. Theodorou's dissertation (Theodorou, 2013) contains estimates of the CO₂ storage capacity of saline formations and depleted petroleum reservoirs in the geologic formation known as "Citronelle Dome," north of Mobile, AL, estimates of CO₂-enhanced oil recovery potential, and calculations of the distribution of CO₂ among supercritical, solution, and mineral phases during and following CO₂ injection into the saline formation separating the two hydrocarbon-bearing zones at Citronelle.

The Research Experience in Carbon Sequestration 2013 (RECS 2013) for graduate students and young professionals in the CCS field (Tomski, 2013, <http://www.recSCO2.org/>), was hosted by Southern Company in Birmingham for the third year in a row, from June 17 to 25, 2013. Please see the information on the RECS program in the paragraph on RECS 2011, on the page after next. There were 27 participants in 2013. Mr. Chris Hobson, Senior Vice President and Chief Environmental Officer of Southern Company Services, gave the Keynote Address, entitled "Utility Perspectives on Energy, Climate & Technology." Richard Esposito gave presentations on Southern Company's CCUS portfolio and key R&D issues (Esposito, 2013a) and an update on the Plant Barry carbon capture and geologic storage demonstration project (Esposito, 2013b). Peter Walsh hosted a visit by the participants to the Caprock Integrity Laboratory. Konstantinos Theodorou and Corey Shum gave a demonstration, in the UAB VisCube, of an animated 3-D visualization of the evolution of oil, water, and CO₂ saturations in a petroleum reservoir during CO₂-EOR.

Michael Hannon gave a poster presentation of his work, entitled "Sensitivity Analyses of a Fully Immersed Pressure-Pulse Decay Experiment on Cylindrical Samples of Layered Porous Media," at the Inverse Problems Symposium in Huntsville, AL, June 9-11, 2013 (Hannon, 2013). The poster described the motivation for Mr. Hannon's work in the need for more rapid and more accurate determination of the permeability of seal layers counted upon to prevent upward migration of CO₂ from storage reservoirs. The presentation included the model that Mr. Hannon has developed for fully-immersed pressure-pulse decay and examples of his parameter estimation procedure and sensitivity analysis.

Senior/Key Co-Investigator Richard Esposito presented a paper, with coauthors C. Harvick, R. Shaw, D. Mooneyhan, R. Trautz, and G. Hill, at the 11th International Conference on Greenhouse Gas Technologies in Kyoto, November 18-22, 2012, entitled, "Integration of Pipeline Operations Sourced with CO₂ Captured at a Coal-Fired Power Plant and Injected for Geologic Storage: SECARB Phase III CCS Demonstration" (Esposito et al., 2013). The paper includes a detailed account of the planning, permitting, and start-up of the SECARB Phase III Plant Barry-Citronelle CCS Project.

The Principal Investigator presented a progress report on the project in the Session, "Geologic Storage 4," at the Carbon Storage R&D Project Review Meeting, "Developing the Technologies and Building the Infrastructure for CCUS," in Pittsburgh on August 22, 2012.

The Research Experience in Carbon Sequestration 2012 (RECS 2012) for graduate students and young professionals in the CCS field (Tomski, 2013, <http://www.recsco2.org/>), was hosted by Southern Company in Birmingham for the second year in a row, from June 3 to 13, 2012. Please see the information on the RECS program in the paragraph on RECS 2011, on the following page. There were 32 participants in 2012. Richard Esposito gave the opening presentation, on Southern Company's CCUS Portfolio and Key R&D Issues (Esposito, 2012). Peter Walsh hosted a visit by the participants to the Caprock Integrity Laboratory and made a presentation on CO₂-enhanced oil recovery from the Citronelle, Alabama, Oil Field (Walsh et al., 2012). Corey Shum and Konstantinos Theodorou gave a demonstration, in the UAB VisCube, of an animated 3-D visualization of the evolution of oil, water, and CO₂ saturations in a petroleum reservoir during CO₂-EOR.

Alan Franks, a student in the Master of Fine Arts Program for Science and Natural History Filmmaking at Montana State University, made several visits to Southern Company, Alabama Power Company, and UAB in March 2012, to shoot a video, entitled "Collaborative Science," documenting the work on carbon capture and storage being done in collaboration with the program in biomineralization at Montana State University (Franks, 2012). The video was screened at the Imagine Science Film Festival in Dublin in July 2012, and it was a finalist in the Scinema Festival of Science Film in Australia. The 10-minute video can be viewed on-line at <<http://vimeo.com/42147696>>.

Michael Hannon was awarded Second Place for his presentation entitled: "Simultaneous Determination of Porosity and Anisotropic Permeability of Cylindrical Core Shale Samples," at the Competition for Doctoral Students on February 23, 2012, during Graduate Student Research Days, the annual symposium for presentation of research by UAB graduate students.

Richard Esposito gave a seminar to students and faculty in the Interdisciplinary Engineering Program and Department of Mechanical Engineering on September 9, 2011, entitled: "Electric Utility Perspectives on Research & Development Required for Commercialization of Carbon Capture and Storage." The seminar was in the weekly series whose purpose is to acquaint advanced undergraduate students, graduate students, and faculty with important research in progress at other organizations and institutions.

Southern Company hosted a visit to the National Carbon Capture Center and UAB on June 16-17, 2011, by representatives from the Georgia Public Service Commission, Georgia Power Company, the Alabama Public Service Commission, and Alabama Power Company. The visit to UAB included a presentation by Richard Esposito, a tour of the Caprock Integrity Laboratory led by Michael Hannon, and a tour of the Visualization Laboratory led by Corey Shum and Bharat Soni.

The Research Experience in Carbon Sequestration 2011 (RECS 2011) was hosted by Southern Company in Birmingham from June 5 to 15, 2011. RECS 2011 was a collaboration between EnTech Strategies, SECARB-Ed, and Southern Company, with sponsorship from the U.S. Department of Energy, Office of Fossil Energy and National Energy Technology Laboratory. The RECS program, founded and directed by Pamela Tomski, fosters and advances education, scientific research, professional training, and career networks for graduate students and young professionals in the CCS field (Tomski, 2013, <http://www.recSCO2.org/>). There were 32 participants in 2011, selected from a much larger pool of applicants. Many of the seminars and exercises in the 2011 program were held at UAB, including a visit by the participants to the Caprock Integrity Laboratory.

Honors student Aaron Lamplugh presented a poster on his independent study project, "Sealing Capacity of Confining Layers," at UAB EXPO, the University's Annual Exposition of Undergraduate Scholarship, on April 22, 2011. Mr. Lamplugh's presentation was awarded Third Place and the award for "Most Interesting Graphics on Poster" in the Engineering Competition Area.

President JianMin Liu and Vice President Xiaoming Wang, from the State Power Environmental Protection Research Institute, based in Nanjing, China, visited UAB and Southern Company on March 13-14, 2011. That visit was a follow-up to the visit by a delegation from the State Power Environmental Protection Research Institute to UAB, Southern Company, the National Carbon Capture Center, Alabama Power Plant Barry, and Gulf Power Plant Crist on October 12-16, 2010, to learn about work being done by Southern Company, Southern Company's operating units, and UAB on carbon capture and sequestration, and to explore possibilities for collaboration in training and research.

The Principal Investigator presented the project by WebEx at the DOE-ARRA Geologic Sequestration Training and Research 2011 Yearly Review Meeting on February 23, 2011.

A paper by Richard Esposito, with coauthors L. S. Monroe and J. S. Friedman, entitled, "Deployment Models for Commercialized Carbon Capture and Storage," was published in the January 1, 2011, issue of *Environmental Science & Technology* (Esposito et al., 2011a). The paper describes and compares infrastructure-based (pipeline) and dispersed-plant options for physical deployment of carbon capture and storage and "self-build and operate," "joint-venture," and "pay at the gate" business models that electric utilities may choose to adopt for management and sequestration of carbon dioxide from combustion of fossil fuels. The abstract from the paper was included in the October 2010 issue of the NETL *Carbon Sequestration Newsletter* (p. 4). Another paper by Dr. Esposito, with coauthors R. Rhudy, R. Trautz, G. Koperna, and G. Hill, entitled, "Integrating Carbon Capture with Transportation and Storage," was presented at the

10th International Conference on Greenhouse Gas Control Technologies in Amsterdam and published in *Energy Procedia* (Esposito et al., 2011b). The latter paper discusses the unique aspects of the integration of carbon dioxide capture at electric power plants with pipeline transport and injection into saline formations. It includes a detailed discussion of the planned demonstration of CO₂ capture from Alabama Power Company's Plant Barry, transport of the CO₂ by pipeline to the Citronelle Oil Field in Southwest Alabama, and sequestration of the CO₂ in a saline formation in Citronelle Dome.

Richard Esposito presented and successfully defended his doctoral dissertation in Interdisciplinary Engineering, entitled: "Business Models for Commercial-Scale Carbon Dioxide Sequestration; with Focus on Storage Capacity and Enhanced Oil Recovery in Citronelle Dome," on November 5, 2010 (Esposito, 2010).

Peter Walsh and Richard Esposito attended the Ninth Annual Conference on Carbon Capture & Sequestration in Pittsburgh, PA, May 10-13, 2010. Dr. Walsh presented a paper, with coauthors K. Theodorou, A. M. Shih, P. C. Shum, G. N. Dittmar, T. Boelens, S. Walker, T. Miller, M. Sullivan, J. C. Pashin, D. J. Hills, D. C. Kopaska-Merkel, R. A. Esposito, E. Z. Nyakatawa, L. J. Lyte, K. A. Roberts, X. Chen, E. S. Carlson, F. Dumkwu, C. A. Turmero, P. E. Clark, S.-E. Chen, Y. Liu, and W. Qi, entitled: "Carbon-Dioxide-Enhanced Oil Recovery and Sequestration in Citronelle Dome, Southwest Alabama." The paper described the pilot test of CO₂-enhanced oil recovery underway in the Citronelle Oil Field in collaboration with Denbury Resources and Southern Company, and the prospects for geologic sequestration of CO₂ in saline formations above the hydrocarbon-bearing zones in Citronelle Dome. This work was also documented in a paper by Dr. Esposito and his coworkers in the journal *Environmental Earth Sciences* (Esposito et al., 2010).

Project Manager Brian Dressel prepared the NETL Fact Sheet for the project in May 2010. <<http://www.netl.doe.gov/publications/factsheets/project/FE0002224.pdf>>

The Project Kick-off Meeting was held via Webex and teleconference on January 14, 2010. The following suggestions were received by the Principal Investigator from the NETL participants in the meeting: (1) Include oxy-combustion among the topics covered in the coal utilization, climate change, and carbon sequestration course, (2) Bring invited speakers in to lecture on their areas of expertise, and (3) Report to NETL the number of students enrolled in the course.

Carla Davis, Communications Specialist in the Public Relations Office at Alabama Power Company, an operating unit of Southern Company, wrote a story announcing the project for the November 23, 2009, issue of *Powergrams*, the news and information publication for Alabama Power Company employees. Following are some quotes from the story, entitled: "Southern Company is leading the way in preparing university students for a future in a brand-new field – clean coal technology operations:"

"Southern Company is collaborating with the University of Alabama at Birmingham (UAB) School of Engineering to introduce students to new technologies that will help reduce greenhouse gas emissions through the capture

and permanent storage, or sequestration, of carbon dioxide (CO₂). The U.S. Department of Energy (DOE) is funding this project to encourage industries and universities to work together to further the development of carbon capture and sequestration technologies.

'If we are going to use this technology commercially, we're going to need a qualified workforce prepared to deploy it,' said Richard Esposito, research geologist, Research and Technology Management, Southern Company Services. 'The DOE recognizes we're moving forward very quickly and that we expect to deploy this technology in the 2020's. That's why we will need employees who have a background in this technology and can design, manage, and operate these systems.'

'Through this partnership, we're able to develop a relationship between us and UAB students so when we actually launch these technologies full-time, we'll have a pool of trained people,' said Research and Technology Management Director Steve Wilson. 'By having UAB faculty and students studying and researching these technologies, it will benefit not only Southern Company, but all electric utilities. The more people focused on the issue, the quicker we can deploy the technology.'

The Media Relations Office at UAB posted a story, entitled: "UAB, Partners Seek Safe Carbon Dioxide Storage for 'Greener' Power Generation," on November 6, 2009, announcing the project on its web site at <<http://www.uab.edu/newsarchive/70807>>.

Southern Company, who provided the services of Senior/Key Co-Investigator Richard Esposito and substantial cost share for the project, issued a press release announcing the award on October 6, 2009, entitled: "Southern Company, University of Alabama at Birmingham to Partner on Greenhouse Gas Reduction Project." <<http://southerncompany.mediaroom.com/index.php?s=43&item=1970>>

Conclusion

Measurement of Rock Properties. The "Caprock Integrity Laboratory," established with support from the present project, is fully functional and equipped for measurement of porosity, permeability, minimum capillary displacement pressure, and effective permeability to gas in the presence of brine. Measurements are made at ambient temperature and under reservoir conditions, with supercritical CO₂. During the course of the project, properties of 19 samples provided by partners on companion NETL projects were measured, covering a range of permeabilities from 0.28 mdarcy to 81 mdarcy.

At the outset of the project, test cells were assembled from 1-inch pipe and compression fittings to hold core sample plugs 7/8" to 1" in diameter. The pipe nipple at the center of the cell was bored out to accept the rock sample and the sample was sealed inside the nipple using epoxy cement (Sadler, Rahnema, and Whittle, 1992). This arrangement worked quite well, was not difficult to assemble, was inexpensive, and provided useful, reproducible data on the first rock samples received at the lab. The value of this approach was that it provided time in which to gain experience with rock measurements, while determining the specifications for a triaxial core holder that would become the workhorse for the experimental work. The simple cell did have several disadvantages: (1) the sample was unavailable for other measurements, outside the cell, having been cemented in place, (2) no axial or radial overburden pressures could be applied to the sample, (3) the pressure difference that could be imposed across the sample was limited by the rock sample strength (not, in our experience, by the strength of the epoxy), and (4) the triaxial core holder is, in fact, much more convenient to use, for its ease of changing samples and obtaining leak-tight set-ups.

Some of the measurements that are being made in the Caprock Integrity Laboratory, such as porosity and absolute permeability, are available at commercial laboratories. The unique aspect of our measurements is that we are in constant communication with the partners who have provided the samples and able to adapt the conditions and procedures of the measurements to their special requirements, as the properties and behavior of the samples become apparent, as work with their samples progresses.

Simulation of CO₂ Migration and Trapping. Reservoir simulations were performed for injection of 530,000 tonnes of CO₂ through a single well into the Middle Donovan formation at Citronelle, Alabama, over 40 years, followed by migration and storage for 10,000 years, using the TOUGHREACT software package from LBNL (Xu, Sonnenthal, Spycher, and Pruess, 2004b, 2004c). It was estimated that 50 kg CO₂/m³ of formation would be converted to minerals within a CO₂ plume approximately 1500 m in diameter during that time.

Sealing Capacity of Caprocks. Citronelle Dome, in northern Mobile County, is the location of Alabama's most productive oil field and an attractive site for CO₂-enhanced oil recovery and CO₂ sequestration. The CO₂ storage capacities of saline formations in Citronelle

Dome were estimated by Esposito et al. (2008). During the present project, the thicknesses of sands thought to be good candidates for CO₂ storage were compared with estimates of their critical CO₂ column height (Berg, 1975), the depth of the layer of CO₂ at which the excess pressure at the top of its column would equal the breakthrough pressure for the confining layers separating the sands.

Estimates of the critical CO₂ column heights ranged from 95 to 120 m. Sand units in the Rodessa formation, about which most is known, because it contains the hydrocarbon-bearing sands, are typically between 2.4 and 12.2 m thick, separated by shale (Esposito et al., 2008). On the basis of the present estimates of critical CO₂ column heights, leakage of CO₂ through those shales is not expected. Even the CO₂ column in the thickest of the sands under consideration, if filled with CO₂ to its full depth of 91 m (Esposito et al., 2008, Figure 5), would not exceed its estimated critical height. Improvement of the model, by more accurate assessment of pore radii, especially in the shales, is recommended.

Simulation of CO₂ Leakage through Caprocks. A model for CO₂ leakage through seal layers by capillary flow, at pressures above the minimum capillary displacement pressure, was based on work by Hildenbrand and coworkers (2004), including a functional relationship between capillary pressure and the effective permeability to gas in the presence of a wetting phase. Under the conditions investigated, with a maximum CO₂ column height of 54 m, doubling the absolute permeability of a 5-m-thick seal layer from 1 to 2 μdarcy, increased CO₂ loss by leakage over 100 years by a factor of five, from 0.8 to 4.1% of the CO₂ injected. Under the same conditions, no leakage by capillary flow was expected through a uniform seal having an absolute permeability of 0.5 μdarcy, in the absence of fractures.

Student Training through Research. At this stage in the development and commercialization of CCUS, there is no shortage of interesting and important questions upon which to base research projects. Four graduate students and one undergraduate student participated in the project. Two were awarded Ph.D. degrees for their work. A third graduate student has proposed research on an advanced technique for measurement of porosity and permeability, and has been admitted to candidacy for the Ph.D. The fourth graduate student is preparing his proposal for research on CCUS and solid waste management. The undergraduate student performed experimental measurements on rock samples and graduated with a B.S. in Mechanical Engineering.

Student Training through Formal Course Work. A course on the application of combustion for electric power generation, focused on pulverized coal combustion, has been offered in the Department of Mechanical Engineering since 2005. Under the present project, the course was augmented with material on climate change, coal gasification, and carbon sequestration. A total of 49 students completed the course during two offerings, in Fall 2010 and Fall 2012. It has become a popular advanced elective course in the Department of Mechanical Engineering. The recent shift by electric utilities from coal to natural gas suggests that future offerings of the course should place more emphasis on natural gas combined cycle power systems.

Acronyms and Symbols

a	ratio of pore volume in a specimen to the upstream chamber volume, Equation 1.2.2, dimensionless
A	cross-section area of the sample perpendicular to the flow direction, m^2
b	ratio of pore volume in a specimen to the downstream chamber volume, Equation 1.2.2, dimensionless
B_V	second Virial coefficient, in the expansion of the compressibility factor, PV , of a gas in powers of $1/V$ (Sengers et al., 1972), $m^3/kmol$
c	isothermal compressibility, Pa^{-1} (Lemmon et al., 2007)
CCS	carbon capture and storage
CCUS	carbon capture, utilization, and storage
D	core sample diameter, m
D_{cap}	grain diameter in caprock, m
D_e	effective grain size, Equation (3.2.3), (Berg, 1975), m
D_{res}	grain diameter in reservoir rock, m
DOE	U.S. Department of Energy
EOR	enhanced oil recovery
$f(a,b)$	function defined by Equation (1.2.2), dimensionless
g	acceleration due to gravity, m/s^2
k	coefficient of permeability, m^2 or darcy
k_{eff}	effective permeability to gas in the presence of a wetting phase, Equation (1.6.1), m^2 or darcy
$k_{eff,max}$	maximum effective permeability to gas in the presence of a wetting phase, Equation (3.3.3), m^2 or darcy
k_r	permeability in the radial direction, parallel to bedding, m^2 or darcy
k_x	permeability in the axial direction, perpendicular to bedding, m^2 or darcy
L	length of a cylindrical core sample, m
LBNL	Lawrence Berkeley National Laboratory, Berkeley, CA
m	van Genuchten (1980) parameter characterizing the spread of a pore size distribution, dimensionless
\dot{m}	mass flow rate, kg/s
N	number of molecules, kmol
NETL	National Energy Technology Laboratory
p	excess pressure imposed by a column of CO_2 beneath a seal, Equation (3.3.2); capillary pressure; internal pore pressure, Equation (2.1.1), Pa

p_0	initial equilibrium pressure, Equation (2.1.2), Pa
p_d	minimum capillary displacement pressure (Hildenbrand et al., 2002, 2004), Pa
p_{max}	capillary pressure at which the maximum effective permeability is reached, Equation (3.3.3), Pa
p_p	pulse pressure, Equation (2.1.2), Pa
p_r	reservoir pressure, Equation (2.1.5), Pa
p_1	instantaneous absolute pressure in the upstream chamber, Equations (1.2.1, 1.6.1), Pa
$p_{1,0}$	initial absolute pressure in the upstream chamber, Equation (1.2.1), Pa
p_2	instantaneous absolute pressure in the downstream chamber, Equations (1.2.1, 1.6.1), Pa
$p_{2,0}$	initial absolute pressure in the downstream chamber, Equation (1.2.1), Pa
P	absolute pressure, Pa
P_e	absolute pressure of gas at the exit from the sample, Equations (1.4.1, 1.5.1), Pa
P_i	absolute pressure of gas at the inlet to the sample, Equations (1.4.1, 1.5.1), Pa
Q	volumetric flow rate of gas, m^3/s
Q_e	volumetric flow rate of gas at the exit from the sample, Equations (1.4.1, 1.5.1), m^3/s
r	radial coordinate in a cylindrical core sample, m
$r_{p,res}$	radius of pores in reservoir rock, Equation (3.2.2) (Graton and Fraser, 1935), m
$r_{t,cap}$	radius of pore throats in caprock, Equation (3.2.2) (Graton and Fraser, 1935), m
R	universal gas constant, = 8314.46 J/(kmol·K); core sample radius, m
s	slope of the line in the plot of the logarithm of dimensionless pressure versus time, Equation (1.2.3), s^{-1}
SECARB	Southeast Regional Carbon Sequestration Partnership
t	time, s
t_n	time at last data point, s
T	absolute temperature, K
TOUGH	Transport of Unsaturated Groundwater and Heat (Pruess et al., 1999; Pruess, 2005; Pruess and Spycher, 2006; Xu et al., 2004a, 2004b, 2004c)
UAB	University of Alabama at Birmingham, Birmingham, AL
V	volume, m^3
V, V_B	bulk volume of the specimen, m^3
V_r	reservoir volume, Equation (2.1.5), m^3
V_1	volume of the upstream chamber, m^3
V_2	volume of the downstream chamber, m^3
W	molecular weight, kg/kmol
x	axial coordinate in a cylindrical core sample, m
\mathbf{X}	parameter sensitivity matrix, Section 2.2
z	gas compressibility factor, dimensionless

z_r	reservoir gas compressibility factor, Equation (2.1.5), dimensionless
γ	surface tension of brine against CO ₂ (Chalbaud et al., 2009), N/m
γ_r	ratio of reservoir volume to pore volume, dimensionless
Δ^n	optimization criterion for parameter estimation, Section 2.2, dimensionless
Δt	time interval corresponding to a change in upstream pressure, Δp_i , s
μ	absolute viscosity of gas at the temperature and mean pressure in the sample (Lemmon et al., 2007), Pa·s
μ_r	absolute viscosity of reservoir gas, Equation (2.1.5), Pa·s
ρ	density, kg/m ³
ρ_{brine}	density of formation water under reservoir conditions, kg/m ³
ρ_{CO_2}	density of carbon dioxide under reservoir conditions (Lemmon et al., 2007), kg/m ³
$\rho_{i,j}$	correlation coefficient between parameters i and j , Figure 2.2.2, dimensionless
σ	standard deviation of the measurement data, Pa
φ, ϕ	porosity, dimensionless

Subscripts

B	bulk (volume)
i, j	parameter indices
in	at the inlet to the sample
n	number of data points
out	at the outlet from the sample
p	pulse (pressure)
r	radial, reservoir
x	axial
0	initial (pressure)

Superscripts

m	number of parameters
n	number of data points

References

American Petroleum Institute, "Recommended Practices for Core Analysis," Recommended Practice 40, 2nd ed., Washington, DC, February 1998.

American Society for Testing and Materials, "Standard Test Method for Permeability of Rocks by Flowing Air," D4525-08, ASTM International, West Conshohocken, PA, 2008.

Beck, J. V., and K. J. Arnold, *Parameter Estimation in Engineering and Science*, John Wiley & Sons, New York, NY, 1977.

Berg, R. R., "Capillary Pressures in Stratigraphic Traps," *AAPG Bulletin*, **1975**, 59 (6), 939-956.

Bikkina, P. K., "Contact angle measurements of CO₂-water-quartz/calcite systems in the perspective of carbon sequestration," *International Journal of Greenhouse Gas Control*, **2011**, 5, 1259-1271.

Brace, W. F., J. B. Walsh, and W. T. Frangos, "Permeability of granite under high pressure," *Journal of Geophysical Research*, **1968**, 73 (6), 2225-2236.

Carslaw, H. S., and J. C. Jaeger, *Conduction of Heat in Solids*, 2nd ed., Oxford University Press, Oxford, 1959.

Chalbaud, C., M. Robin, J.-M. Lombard, F. Martin, P. Egermann, and H. Bertin, "Interfacial tension measurements and wettability evaluation for geological CO₂ storage," *Advances in Water Resources*, **2009**, 32, 98-109.

Chiquet, P., D. Broseta, and S. Thibeau, "Wettability alteration of caprock minerals by carbon dioxide," *Geofluids*, **2007**, 7, 112-122.

Collins, R. E., *Flow of Fluids through Porous Materials*, PennWell Publishing Co., Tulsa, OK, 1961, pp. 50-51.

Dicker, A. I., and R. M. Smits, "A Practical Approach for Determining Permeability from Laboratory Pressure-Pulse Decay Measurements," Paper No. SPE 17578, Society of Petroleum Engineers, Richardson, TX, 1988.

Ellison, K. M., "Risks posed to drinking water aquifers due to leakage of dissolved CO₂ in improperly abandoned wellbores," M.S. Thesis, Clemson University, 2011, 82 pages.

Espinoza, D. N., and J. C. Santamarina, "Water-CO₂-mineral systems: Interfacial tension, contact angle, and diffusion - Implications to CO₂ geological storage," *Water Resources Research*, **2010**, *46*, W07537, doi:10.1029/2009WR008634.

Esposito, R. A., "Business Models for Commercial-Scale Carbon Dioxide Sequestration; with Focus on Storage Capacity and Enhanced Oil Recovery in Citronelle Dome," Doctoral Dissertation, Interdisciplinary Engineering, University of Alabama at Birmingham, 2010.

Esposito, R. A., "One Great Team: Southern Company Generation, Clean Coal Technology Development," Research Experience in Carbon Sequestration 2012, Birmingham, AL, June 3-13, 2012.

Esposito, R. A., 2013a, "Update on Southern Company's Carbon Capture and Geologic Storage R&D Projects," Research Experience in Carbon Sequestration 2013, Birmingham, AL, June 17-25, 2013.

Esposito, R. A., 2013b, "Update on the Plant Barry Carbon Capture and Geologic Storage Demonstration Project," Research Experience in Carbon Sequestration 2013, Birmingham, AL, June 17-25, 2013.

Esposito, R. A., J. C. Pashin, and P. M. Walsh, "Citronelle Dome: A Giant Opportunity for Multi-Zone Carbon Storage and Enhanced Oil Recovery in the Mississippi Interior Salt Basin of Alabama," *Environmental Geosciences*, **2008**, *15* (2), 53-62.

Esposito, R. A., J. C. Pashin, D. J. Hills, and P. M. Walsh, "Geologic assessment and injection design for a pilot CO₂-enhanced oil recovery and sequestration demonstration in a heterogeneous oil reservoir: Citronelle Field, Alabama, USA," *Environmental Earth Sciences*, **2010**, *60*, 431-444.

Esposito, R. A., L. S. Monroe, and J. S. Friedman, 2011a, "Deployment Models for Commercialized Carbon Capture and Storage," *Environmental Science & Technology*, **2011**, *45* (1), 139-146.

Esposito, R., R. Rhudy, R. Trautz, G. Koperna, and G. Hill, 2011b, "Integrating Carbon Capture with Transportation and Storage," *Energy Procedia*, **2011**, *4*, 5512-5519.

Esposito, R., C. Harvick, R. Shaw, D. Mooneyhan, R. Trautz, and G. Hill, "Integration of Pipeline Operations Sourced with CO₂ Captured at a Coal-Fired Power Plant and Injected for Geologic Storage: SECARB Phase III CCS Demonstration," 11th International Conference on Greenhouse Gas Technologies, Kyoto, Japan, November 18-22, 2012. *Energy Procedia*, **2013**, *37*, 3068-3088.

Finsterle, S., and P. Persoff, "Determining permeability of tight rock samples using inverse modeling," *Water Resources Research*, **1997**, *33* (8), 1803-1811.

Franks, A., "Collaborative Science," Science and Natural History Filmmaking, Montana State University, Bozeman, MT, 10-minute video, 2012, <<http://vimeo.com/42147696>>

Graton, L. C., and H. J. Fraser, "Systematic Packing of Spheres with Particular Relation to Porosity and Permeability," *The Journal of Geology*, **1935**, 43 (8), 785-909.

Hannon, M. J., Jr., "Sensitivity Analyses of a Fully Immersed Pressure-Pulse Decay Experiment on Cylindrical Samples of Layered Porous Media," Poster presentation at the 2013 Inverse Problems Symposium, Huntsville, AL, June 9-11, 2013.

Haskett, S. E., G. M. Narahara, and S. A. Holditch, "A method for simultaneous determination of permeability and porosity in low-permeability cores," *Society of Petroleum Engineers Formation Evaluation*, **1988**, 3 (3), 651-658.

Hildenbrand, A., S. Schlömer, and B. M. Krooss, "Gas breakthrough experiments on fine-grained sedimentary rocks," *Geofluids*, **2002**, 2, 3-23.

Hildenbrand, A., S. Schlömer, B. M. Krooss, and R. Littke, "Gas breakthrough experiments on pelitic rocks: comparative study with N₂, CO₂ and CH₄," *Geofluids*, **2004**, 4, 61-80.

Hsieh, P. A., J. V. Tracy, C. E. Neuzil, J. D. Bredehoeft, and S. E. Silliman, "A transient laboratory method for determining the hydraulic properties of 'tight' rocks - I. Theory," *International Journal of Rock Mechanics and Mining Sciences & Geomechanics Abstracts*, **1981**, 18 (3), 245-252.

Klinkenberg, L. J., "The Permeability of Porous Media to Liquids and Gases," *Drilling and Production Practice*, American Petroleum Institute, Washington, DC, 1941, pp. 200-213.

Kvamme, B., T. Kuznetsova, A. Hebach, A. Oberhof, and E. Lunde, "Measurements and modelling of interfacial tension for water + carbon dioxide systems at elevated pressures," *Computational Materials Science*, **2007**, 38, 506-513.

Lamplugh, A. D., "Sealing Capacity of Confining Layers," Poster presentation at UAB EXPO, An Exposition of Undergraduate Scholarship, University of Alabama at Birmingham, Birmingham, AL, April 22, 2011.

Lemmon, E. W., M. L. Huber, and M. O. McLinden, "REFPROP Reference Fluid Thermodynamic and Transport Properties," NIST Standard Reference Database 23, Version 8.0, Physical and Chemical Properties Division, U.S. Department of Commerce, 2007.

Ning, X., "The Measurement of Matrix and Fracture Properties in Naturally Fractured Low Permeability Cores Using a Pressure Pulse Method," Doctoral Dissertation, Petroleum Engineering, Texas A&M University, College Station, TX, 1992.

Phillips, A. J., "Biofilm-Induced Calcium Carbonate Precipitation: Application in the Subsurface," Dissertation, Doctor of Philosophy in Engineering, Montana State University, Bozeman, MT, 2013.

Pruess, K., "ECO2N: A TOUGH2 Fluid Property Module for Mixtures of Water, NaCl, and CO₂," Report No. LBNL-57952, Lawrence Berkeley National Laboratory, Berkeley, CA, August 2005.

Pruess, K., and N. Spycher, "ECO2N – A New TOUGH2 Fluid Property Module for Studies of CO₂ Storage in Saline Aquifers," Proceedings, TOUGH Symposium 2006, Report No. LBNL-60072, Lawrence Berkeley National Laboratory, Berkeley, California, May 15–17, 2006.

Pruess, K., C. Oldenburg, and G. Moridis, "TOUGH2 User's Guide, Version 2.0," Report No. LBNL-43134, Lawrence Berkeley National Laboratory, Berkeley, CA, November 1999.

Sadler, L. Y., M. B. Rahnema, and G. P. Whittle, "Laboratory Measurement of the Permeability of Selma Chalk Using an Improved Experimental Technique," *Hazardous Waste & Hazardous Materials*, **1992**, 9, 331-343.

Sengers, J. M. H. L., M. Klein, and J. S. Gallagher, "Pressure-Volume-Temperature Relationships of Gases; Virial Coefficients," Section 4i in: Gray, D. E. (Ed.), *American Institute of Physics Handbook*, 3rd ed., McGraw-Hill, New York, 1972, pp. 4-204 to 4-221.

Theodorou, K., "Carbon Dioxide Enhanced Oil Recovery from the Citronelle Oil Field and Carbon Sequestration in the Donovan Sand, Southwest Alabama," Doctoral Dissertation, Interdisciplinary Engineering, University of Alabama at Birmingham, 2013.

Tomski, P., RECS, Research Experience in Carbon Sequestration, 2013, <<http://www.recsco2.org/>>.

van Genuchten, M. T., "A Closed-Form Equation for Predicting the Hydraulic Conductivity of Unsaturated Soils," *Soil Sci. Soc. Am. J.*, **1980**, 44, 892–898.

Walsh, P. M., K. Theodorou, P. C. Shum, E. Z. Nyakatawa, X. Chen, K. A. Roberts, L. J. Lyte, G. N. Dittmar, K. Murphy, S. Walker, T. Boelens, P. Guerra, T. Miller, T. Henderson, M. Sullivan, D. Beasley, S. Brewer, F. Everett, J. C. Pashin, D. J. Hills, D. C. Kopaska-Merkel, R. A. Esposito, K. M. Ellison, E. S. Carlson, P. E. Clark, A. W. Islam, C. A. Turmero, F. Dumkwu, S.-E. Chen, W. Qi, Y. Liu, and P. Wang, "Citronelle Dome, Southwest Alabama: CO₂-Enhanced Oil Recovery Pilot Test and Opportunities for CO₂ Storage," Research Experience in Carbon Sequestration 2012, Birmingham, AL, June 3-13, 2012.

Xu, T., J. A. Apps, and K. Pruess, 2004a, "Numerical simulation of CO₂ disposal by mineral trapping in deep aquifers," *Applied Geochemistry*, **2004**, 19, 917-936.

Xu, T., E. L. Sonnenthal, N. Spycher, and K. Pruess, 2004b, "TOUGHREACT user's guide: A simulation program for non-isothermal multiphase reactive geochemical transport in variable saturated geologic media," Lawrence Berkeley National Laboratory, Report No. LBNL-55460, Berkeley, CA, 2004.

Xu, T., E. Sonnenthal, N. Spycher, and K. Pruess, 2004c, "TOURGHREACT: A Simulation Program for Non-isothermal Multiphase Reactive Geochemical Transport in Variably Saturated Geologic Media," Lawrence Berkeley National Laboratory, Paper No. LBNL-56740, Berkeley, CA, 2004. <http://www.escholarship.org/uc/item/1h55t380>